Dispersal and polyandry evolve as competing inbreeding avoidance strategies

Greta Bocedi[1]

[1]School of Biological Sciences, University of Aberdeen, Zoology Building, Tillydrone Avenue, Aberdeen, AB24 2TZ, UK.

Abstract

Understanding evolution of complex life-histories requires explicitly considering their multiple interactions, feedbacks, and shared drivers. Inbreeding depression is hypothesized to drive evolution of two life-histories which have far-reaching ecological and evolutionary consequence: dispersal and polyandry. Yet, the role of inbreeding depression in the separate evolution of these key life-histories is still debated, while the possibility for their joint evolution and consequent covariation has not been considered. I propose that dispersal and polyandry might be competing means of inbreeding avoidance which negatively feedback on each other's evolution. Using a genetically explicit individual-based model, I first demonstrate that inbreeding depression can drive the separate evolution of dispersal and polyandry. Although this is largely known for dispersal, it is not as well established for polyandry evolution, which generally remains an evolutionary puzzle. Here, I show that polyandry can indeed evolve as means of indirect inbreeding avoidance in spatially structured populations. Second, when dispersal and polyandry can evolve jointly, a negative feedback emerges, such that they evolve as alternative inbreeding avoidance strategies across replicate systems, especially if there are fitness costs associated. Finally, although both dispersal and polyandry might be expected to shape the level of inbreeding depression, this is mainly affected by dispersal, while polyandry has a much more limited effect. These results emphasize the need to consider the potential joint evolution of dispersal and mating system in general, together with their genetic effects, to further our understanding of life-history

evolution in spatially structured systems, and provide theoretical expectations for new empirical testing.

Key words: female multiple mating, dispersal, heterosis, deleterious recessive mutations, genetically explicit modelling

Introduction

Understanding evolution of life-histories and their consequences for populations' ecology and evolution ultimately requires recognizing the multiple interactions, such as feedbacks, tradeoffs, and shared drivers, existing among different strategies and between potentially competing resolutions of fitness costs. Although most often evolution of different traits is being treated separately, comprehensive understanding of how life-histories evolve under different environmental circumstances, including environmental changes, requires joint evolutionary dynamics to be elucidated. One prominent example is the evolution of competing mechanisms of inbreeding avoidance (Szulkin et al. 2013; Duthie et al. 2018), and specifically the potential for the joint evolution of dispersal and polyandry as competing responses to inbreeding depression, which could then feedback to shape the population's genetic load and consequent fitness. Yet, such joint evolutionary dynamics have not been examined, precluding comprehensive predictions of mating system evolution in spatially structured populations, as well as its genetic implications.

Inbreeding depression, defined as the reduction in fitness components of offspring of related individuals compared to offspring of unrelated individuals, is a widespread phenomenon that has profound demographic and evolutionary consequences (Keller and Waller 2002; Charlesworth and Willis 2009). It can reduce the mean fitness of a population and increase extinction risk (Theodorou and Couvet 2006; Hedrick and Garcia-Dorado 2016), and it can affect trait evolution (Lande and Schemske 1985; Charlesworth and Charlesworth 1987; Szulkin et al.

2013). Inbreeding depression is widely hypothesized to be a key driver of the evolution of two potential inbreeding avoidance mechanisms, dispersal and polyandry, which play a central role in populations' ecological and evolutionary dynamics, as they both shape gene flow within and between populations (Waser et al. 1986; Stockley et al. 1993; Perrin and Mazalov 1999; Jennions and Petrie 2000; Tregenza and Wedell 2002). Dispersal, that is any individual movement potentially leading to spatial gene flow (Ronce 2007; Clobert et al. 2012), shapes populations' spatiotemporal structure as well as their genetic structure, and the extent and direction of gene flow among populations (Clobert et al. 2012). Polyandry, defined as female mating with multiple males within a single reproductive bout (Pizzari and Wedell 2013; Taylor et al. 2014), has only more recently been recognized to have far reaching evolutionary and ecological consequences, and yet remains an evolutionary puzzle (Holman and Kokko 2013; Kvarnemo and Simmons 2013; Pizzari and Wedell 2013). In turn, both dispersal and polyandry can change the relatedness structure within and among populations, thus affecting opportunity for inbreeding and consequent evolution of inbreeding depression (Ronce 2007; Germain et al. 2018).

Despite inbreeding depression being a potential major shared driver, and despite the large amount of both theoretical and empirical work, evolution of dispersal and polyandry given inbreeding have been so far studied separately. Thus, we still do not know whether and how dispersal and polyandry affect each other's evolution, and how they may feed back onto evolution of inbreeding depression itself. Filling this knowledge gap is particularly important because populations exist in space and it is unlikely that major life-histories, such as dispersal and mating system, evolve independently (Ronce and Clobert 2012; Auld and Rubio de Casas 2013; Hargreaves and Eckert 2014). Further, ongoing environmental changes, such as habitat fragmentation and isolation, are fragmenting populations in smaller demes thus increasing the risk of inbreeding, and more generally demanding understanding of eco-(co-)evolutionary

74 dynamics of life-histories in highly structured systems (Hanski 2011; Cheptou et al. 2017; Legrand
75 et al. 2017).

76 It is now accepted that inbreeding depression and heterosis (i.e., the increase in fitness in
77 offspring originating from between populations crosses relative to offspring from within population
78 crosses; Charlesworth and Charlesworth 1987; Whitlock et al. 2000; Charlesworth and Willis
79 2009) can drive dispersal evolution, although debate remains on the form and the relative
80 importance of this effect (Perrin and Goudet 2001; Ronce 2007; Szulkin and Sheldon 2008; Pike
81 et al. 2021). Theoretical work has shown inbreeding depression and heterosis can results in
82 substantial evolution of dispersal, which may be sex-biased or equal between the sexes
83 depending on factors such as the cost of dispersal, the type and strength of same sex competition,
84 the mating system, the strength of inbreeding depression and the presence of demographic and
85 environmental stochasticity (Gandon 1999; Perrin and Mazalov 2000; Guillaume and Perrin 2006,
86 2009; Roze and Rousset 2009; Henry et al. 2016; Li and Kokko 2019). Substantial insights have
87 been achieved by theoretical models that consider the joint evolution of dispersal and inbreeding
88 depression. These models do not assume constant inbreeding depression but explicitly model
89 the accumulation and purging of deleterious recessive mutations responsible for inbreeding
90 depression and genetic load more generally (Guillaume and Perrin 2006, 2009; Roze and
91 Rousset 2009; Henry et al. 2016). Particularly, Roze and Rousset (2009) by using a continuous
92 chromosome model, which allows modelling a potentially infinite number of deleterious recessive
93 mutations, showed that heterosis can have a much more important effect (relative to kin
94 competition) on dispersal evolution than previously thought (Guillaume and Perrin 2006; Ravigné
95 et al. 2006), especially when population size is large and the genomic deleterious mutation rate
96 is in the upper range of observed values. Further, the effect of heterosis increases when mutations
97 become more recessive (Guillaume and Perrin 2006; Roze and Rousset 2009). However, even

studies that include a genetically explicit model of inbreeding depression, generally assume a fixed selection coefficient, *s*, and a dominance coefficient, *h*, across deleterious mutations. Thus, we still do not know how a more realistic distribution of deleterious mutations, which likely comprises many mutations with very small fitness effects and rare ones with larger effects (Eyre-Walker and Keightley 2007), and a negative relationship between selection and dominance coefficients (Agrawal and Whitlock 2011; Huber et al. 2018), might impact on evolving inbreeding depression, and the consequent evolution of dispersal and mating systems (Porcher and Lande 2016).

Meanwhile, explaining the evolution and persistence of polyandry is an ongoing pursuit in evolutionary biology, that is especially challenging when there is direct selection against it, that is when polyandry is costly to females (Arnqvist and Nilsson 2000; Jennions and Petrie 2000; Slatyer et al. 2012; Parker and Birkhead 2013). Although the hypothesis that inbreeding depression can drive the evolution of female multiple mating is prominent among the different evolutionary mechanisms that have been postulated, it remains less established in its theoretical and empirical demonstration, compared to dispersal (Stockley et al. 1993; Jennions and Petrie 2000; Tregenza and Wedell 2002; Reid and Sardell 2012; Reid et al. 2015; Duthie et al. 2016; Germain et al. 2018). Polyandry has been hypothesized to evolve as a mechanism for inbreeding avoidance through two main routes: direct or indirect inbreeding avoidance (Germain et al. 2018). Female multiple mating could evolve because it facilitates inbreeding avoidance through female active pre- and/or post-copulatory allocation of paternity to less closely related males, hence directly reducing inbreeding depression in offspring viability (direct inbreeding avoidance) (Jennions and Petrie 2000; Tregenza and Wedell 2002; Duthie et al. 2016, 2018). Alternatively, without invoking active mate choice and kin recognition, polyandry could evolve because it alters relatedness among the female's offspring, producing more half-sibs rather than full-sibs, thereby

122 reducing the risk of close inbreeding for the offspring of a polyandrous female and reducing
123 inbreeding depression in her grand offspring (indirect inbreeding avoidance) (Cornell and
124 Tregenza 2007; Germain et al. 2018). The few theoretical models to have investigated these
125 verbal predictions (Cornell and Tregenza 2007; Duthie et al. 2016, 2018) have generally
126 concluded that the strength of indirect selection on polyandry through inbreeding avoidance might
127 be very small, thereby suggesting a minor role of inbreeding depression in polyandry evolution.

128 Specifically, Cornell and Tregenza (Cornell and Tregenza 2007) concluded that purging
129 of deleterious recessive mutations makes it unlikely to maintain sufficient levels of inbreeding
130 depression to favor costly polyandry, and that the evolution of polyandry as a mechanism of
131 indirect inbreeding avoidance is far more likely if inbreeding depression was due to
132 overdominance. This poses a problem because current understanding suggests that inbreeding
133 depression is predominantly caused by deleterious recessive, rather than overdominant,
134 mutations (Charlesworth and Willis 2009). However, Cornell and Tregenza's (2007) model makes
135 some assumptions that preclude assessing whether such a mechanism could generally drive
136 polyandry evolution in spatially structured populations. The model considers alternating
137 generations of outbreeding and inbreeding, which is particularly relevant to some invertebrate
138 groups where mated females cyclically colonize empty patches, thus experiencing cyclical
139 changes in inbreeding risk (e.g., store product pest species such as flour beetles, *Tribolium* spp.).
140 However, this does not apply to species with more regular inbreeding as it does not consider the
141 building up of complex relatedness structure within a population, that arise across multiple
142 generations and might weaken the selective advantage of polyandry (Germain et al. 2018).
143 Indeed, Cornell and Tregenza's (Cornell and Tregenza 2007) pointed out that higher levels of
144 inbreeding, as we might expect in spatially structured populations, might favor polyandry, although
145 this might be offset by greater purging of deleterious recessives alleles. No model so far has

146 investigated the evolution of polyandry as a mechanism of indirect inbreeding avoidance in
147 populations that are spatially structured and connected by dispersal, nor has considered an
148 explicit model of inbreeding depression with realistic distributions of the fitness effects and
149 dominance coefficients of deleterious mutations, thus leaving a substantial knowledge gap.

150 Beyond the unknowns that are still present in the separate theories of dispersal and
151 polyandry evolution given inbreeding depression, we do not know how these two potential
152 mechanisms of inbreeding avoidance might affect each other's evolution, and feed back onto
153 evolution of inbreeding depression. I hypothesize a negative feedback between dispersal and
154 polyandry, whereby the evolution of polyandry might reduce inbreeding and hence reduce the
155 strength of selection for dispersal and, *vice versa*, the presence of high dispersal might weaken
156 selection for polyandry. The outcome of this tug-o-war will likely depend on the relative efficiency
157 of dispersal and polyandry in reducing inbreeding, with the expectation that dispersal would be
158 much more effective, on the level of inbreeding load, and on the strength of direct selection against
159 them, that is on the cost of dispersal and polyandry.

160 I investigate this hypothesis with a modelling framework that allows joint evolution of
161 dispersal and polyandry in spatially structured populations and, at the same time, explicit
162 accumulation of deleterious mutations and evolution of inbreeding depression. Specifically,
163 inbreeding depression is determined by accumulation of a potentially infinite number of
164 deleterious recessive mutations with a realistic distribution of fitness effects and dominance
165 coefficients. First, I test whether existing predictions on the independent evolution of dispersal
166 and polyandry hold in spatially structured populations given an explicit model of inbreeding and
167 inbreeding depression evolution, and how their evolution affects inbreeding depression. Second,
168 I test the novel hypothesis of a negative feedback between jointly evolving dispersal and
169 polyandry and, third, determine their joint effect on the evolution of inbreeding depression. More

generally, I show the value of moving towards theoretical frameworks that explicitly integrate ecology, genetics, and evolution, to progress our understanding of life-history evolution and its impacts on populations.

The Model

To investigate the joint evolution of dispersal and polyandry given inbreeding depression I built a spatially and genetically explicit individual-based model where emigration probability (d) and female re-mating rate (a) evolve. Genetic load and resulting inbreeding depression (ID) also evolve by accumulation and purging of deleterious recessive mutations. Populations of a dioecious species, with non-overlapping generations, occupy cells within a landscape grid of 20 by 20 cells, and are connected by dispersal. The environment is spatially homogeneous and temporally constant; each cell is suitable to hold a population with constant carrying capacity K = 50. All the model variables and parameters are listed in Table S1.

Genetic architecture and inbreeding depression. To model the genetic basis of d and a, individuals carry two unlinked diploid loci with a continuous distribution of alleles (Kimura 1965). The initial value of each allele is sampled from normal distributions. Alleles can mutate with probability $\mu = 10^{-3}$/allele/generation. When a mutation occurs a random normal deviate with mean zero is added to the allele value. The individual's genotypic values for the two traits, g_d and g_a, are given by the sum of the two allelic values at the respective loci. The phenotypic expression has no environmental variance and is female limited for a. I assume the phenotypes $a \geq 0$ and $0 \leq d \leq 1$.

ID is determined by deleterious recessive mutations (Charlesworth and Willis 2009) which accumulate on a continuous chromosome (Roze and Rousset 2009). Each individual carries two homologous autosomes of length R (genome map length). The position of each new deleterious

mutation on the chromosome is sampled from the continuous uniform distribution $U[0, R]$. The number of loci at which mutations can occur is therefore effectively infinite ("infinite site model" (Peischl et al. 2015)). Each new mutation is characterized by a selection coefficient *s*, determining the mutation's effect in the homozygous state, and a dominance coefficient *h*. The effect of each mutation *i* is multiplicative such that the genetic fitness *ω* of an individual is given by

$$\omega = \prod_{Nhet}(1 - h_i s_i) \prod_{Nhom}(1 - s_i) \quad [1]$$

Nhet and *Nhom* represent the number of heterozygous and homozygous mutations respectively. Deleterious mutations are of two types: mildly deleterious and lethal (Gilbert et al. 2017; Spigler et al. 2017). Mildly deleterious mutations occur at a rate U_d = 1.0/diploid genome/generation (Haag-Liautard et al. 2007; Zhu et al. 2014). The selection coefficient of each new mutation is sampled from a gamma distribution with mean s_d = 0.05 and shape parameter α = 1 (Schultz and Lynch 1997; Spigler et al. 2017). The dominance coefficient of a mutation *i* depends on its selection coefficient s_i and is sampled from the continuous uniform distribution $U[0.0, e^{-ks_i}]$. *k* is defined as $-\log(2h_d)/s_d$, where h_d is the mean dominance coefficient (h_d = 0.3) (Caballero and Keightley 1994; Spigler et al. 2017). Lethal mutations occur at rate U_l = 0.2/diploid genome/generation and are extremely recessive, with constant selection coefficient s_l = 1 and dominance coefficient h_l = 0.02 (Simmons and Crow 1977; Lande et al. 1994; Porcher and Lande 2005; Spigler et al. 2017). At each generation, the number of new mutations per diploid genome is sampled from Poisson distributions with parameters U_d and U_l. The number of crossovers along the continuous chromosomes is sampled from a Poisson distribution with mean *R*, and the position of each crossover is sampled from the uniform distribution $U[0, R]$.

Individuals also carry L_n = 500 neutral autosomal diploid loci to determine the degree to which individuals are inbred (Bocedi and Reid 2017). Neutral allelic values are continuously distributed, sampled from the uniform distribution $U[-1000.0, 1000.0]$, and mutate with probability 10^{-3} /allele/generation. Neutral loci recombine at rate r = 0.1. Alleles at the same locus will be identical only by descent as the chance of non-descent identity by state, stemming from initialization or mutation, is negligible. For this reason, individual's neutral homozygosity, defined as the number of neutral homozygous loci / L_n, represents a proxy for the realized individual coefficient of inbreeding, hereafter noted as F_{homoz} (Markert et al. 2004; Neff and Pitcher 2008; Fromhage et al. 2009; Bocedi and Reid 2017). When an individual is born, it is assumed to die immediately if its genetic fitness ω = 0. If ω > 0, the newborn survives to adulthood (unless it incurs in dispersal mortality, see below) when ω will determine its probability of reproducing. Thus, ID is affecting two fitness components: 1) reduction in offspring survival, which is determined by the presence of homozygous lethal mutations, and 2) reduction in adult probability of reproducing, which is determined mainly by mildly deleterious mutations.

The level of ID present in a metapopulation at a given point in time, was calculated as: 1) effect of F_{homoz} on offspring survival by fitting a generalized linear model with Poisson distribution and logarithmic link function (Nietlisbach et al. 2019); 2) effect of F_{homoz} on the logarithm of adult reproduction probability by fitting a linear model (Morton et al. 1956). All models were fitted in R (R Core Team 2019). To obtain a spread of F_{homoz} values to estimate ID, I created individuals by selecting the central 140 populations in the landscape (out of 400 populations) at a given point in time. For each of these populations, I mated each female with 10 males selected randomly within the female's population and with 10 males selected randomly between different populations. Each mating produced one offspring. Models were then fitted on all the offspring pooled together. These individuals were also used to calculate the level of heterosis (H) in each population as $H = 1 -$

ω_w/ω_b, where ω_w is the genetic fitness of offspring produced within populations, and ω_b is the genetic fitness of offspring produced between populations (e.g., Roze and Rousset 2009). All the offspring produced this way were used only for estimating ID and H, and then discarded, thus were not part of the ecological and evolutionary dynamics.

***Life cycle and selection*.** At each generation, the life cycle consists of reproduction (mating and offspring birth), adults' death and death of offspring with $\omega = 0$, offspring dispersal and density-dependent survival. An adult's probability of reproducing is given by its genetic fitness ω. Each reproducing female *i* mates initially once, and then re-mates with probability $Pmat_i$ depending on her re-mating rate phenotype a_i and on her current number of mates Nm_i:

$$Pmat_i = e^{-a_i Nm_i} \quad [2]$$

Each mate is randomly sampled among the reproducing males in the female's population, without replacement. If the female has already mated once with all the reproducing males in the population, she stops re-mating. Mating multiply can be costly to females. The probability that a female *i* survives to reproduction (ψ_i) depends on her total number of mates $Nmates_i$ and on the strength of selection against multiple mating ω_m^2:

$$\psi_i = e^{-\frac{(1-Nmates_i)^2}{2\omega_m^2}} \quad [3]$$

If the female survives mating, she produces a number of offspring sampled from a Poisson distribution with mean $f = 12$ and primary sex-ratio = 1:1. Each offspring is sired by a male randomly chosen, with replacement, between the female's mates.

After reproduction, all adults die, and offspring may disperse among sub-populations according to their emigration probability phenotype *d*. Dispersal distance and direction are

sampled from a negative exponential distribution (mean 2 cells), and uniform distribution between 0 and 2π, respectively. The new location is re-sampled if it falls outside the grid. Dispersal has a cost, c_d, representing the probability of an individual dying during dispersal. After dispersal, density-dependent survival takes place in each population. Individuals survive with probability $min(K/N, 1)$, where *N* is the total number of individuals in the population.

***Simulations*.** I ran three main sets of simulations. 1) Only dispersal is evolving while female re-mating rate is constant, a = 3 (corresponding to 1.3 mates per female on average – hereafter defined as monandry); 2) only female re-mating rate is evolving while dispersal is constant, d = 0.05; 3) both dispersal and female re-mating rate are evolving. All simulations were run under varying costs of dispersal and female re-mating and repeated in the absence of deleterious mutations (and hence ID) as control. I additionally tested the effect of varying the rates of deleterious mutation (U_d = 0.5 and U_l = 0.1; U_d = 0.1 and U_l = 0.02).

Results and Discussion

***Evolution of dispersal and inbreeding depression given monandry*.** Under fixed monandry conditions, emigration probability d evolved in response to the presence of deleterious recessive mutations and consequent inbreeding depression (ID), reaching higher values the lower the cost of dispersal (c_d; Fig. 1A). Much higher emigration probability evolved in the presence than in the absence of genetic load when, given the spatio-temporally homogeneous environment, the only driver of dispersal evolution was kin competition. For example, at the lower cost considered (c_d = 0.3), d evolved almost eight times higher with ID [median $\bar{d}$ = 0.41 (95%CI 0.401-0.414), where $\bar{d}$ represents the mean phenotypic value for one replicate metapopulation; median and CI are taken across 20 replicates] than without ID [median $\bar{d}$ = 0.05 (95%CI 0.05-0.054)]; while it was almost seven times higher at high cost of dispersal [c_d = 0.6; median $\bar{d}$ = 0.15 (95%CI 0.15-

0.157) with ID *vs*. median $\bar{d}$ = 0.02 (95%CI 0.02-0.023) without ID]. Results remained qualitatively similar under lower rates of deleterious mutations, although the lower the mutation rate the lower the evolved dispersal probability (Fig. S1A-S2A). The level of heterosis H reached at equilibrium depended on the level of evolved dispersal, and hence on dispersal cost (Fig. S3A). Higher cost of dispersal led to lower dispersal and to populations being less homogeneous in terms of their genetic load, and hence to higher heterosis. Higher rates of deleterious mutations, by causing accumulation of higher genetic load, led to the emergence of higher heterosis compared to lower mutation rates. These results broadly agree with the conclusions of Roze and Rousset (2009) who, by using a genetically explicit, infinite site model of genetic load, showed that heterosis can have a substantial role in dispersal evolution, in contrast with what shown by previous models (Guillaume and Perrin 2006; Ravigné et al. 2006). Importantly, the results also show that the qualitative predictions made by (Roze and Rousset 2009) hold when assuming a realistic distribution of mutational effects in terms of selection and dominance coefficients; despite the accumulation of many mutations with very low (almost neutral) selection coefficient, substantial heterosis is maintained as it is its substantial role (relative to kin competition) in driving dispersal evolution.

The level of evolved ID depended on the level of evolved dispersal, and hence on dispersal cost (Fig. 1C-E; Table S2). Higher dispersal cost led to lower *d* and consequent higher inbreeding within local populations, reflected by higher neutral homozygosity (Fig. 1C). In turn, more inbreeding facilitated purging of deleterious recessive mutations thus reducing ID. This was true for both components of ID. Both lethal mutations (strongly recessive mutations causing ID in early life – offspring survival, Fig. 1E) and mildly deleterious mutations (causing ID in later life – adult reproduction probability, Fig. 1C) experienced greater purging at lower dispersal, where both the mutation load (i.e., the decrease in fitness for outbred individuals) and ID were lower compared

306 to scenarios with much higher dispersal evolving, albeit grater differences were observed for ID
307 rather than for mutation load (Table S2). This pattern was conserved at lower mutation rates
308 although much less genetic load accumulated, leading to higher individual fitness and lower
309 mutation and inbreeding load (Fig. S1C-E; S2C-E). There is therefore a positive feedback
310 between evolution of dispersal and inbreeding depression, whereby high dispersal maintains high
311 levels of inbreeding depression, which in turn maintains positive selection for dispersal.

312 ***Evolution of polyandry and inbreeding depression given low dispersal.*** Like dispersal,
313 polyandry (expected female number of matings, $P = 1 + 1/a$) evolved in response to ID when
314 dispersal was low and not evolving, to a level that depended on the fitness cost of female multiple
315 mating (Fig. 1B; Fig. S4). Given no cost of polyandry, females evolved to mate with all the males
316 present in the population. However, even a very small cost reduced substantially $\overline{P}$ (where $\overline{P}$
317 represents the mean phenotypic value for one replicate metapopulation); yet moderate polyandry
318 evolved. For example, strength of direct selection on re-mating ω_m^2= 1000 led to evolution of
319 median $\overline{P}$ = 4.13 (95%CI 3.51-5.26) (median and CI are taken across 20 replicates),
320 corresponding to an average realized survival cost of 0.005 for females. On the contrary, in the
321 absence of ID, polyandry did not evolve even when free of cost (Fig. 1B and S4, dashed lines).
322 Lower rates of mildly deleterious and lethal mutations substantially reduced selection for
323 polyandry such that hardly any polyandry evolved, or evolution took considerably longer time (Fig.
324 S1B; S2B).

325

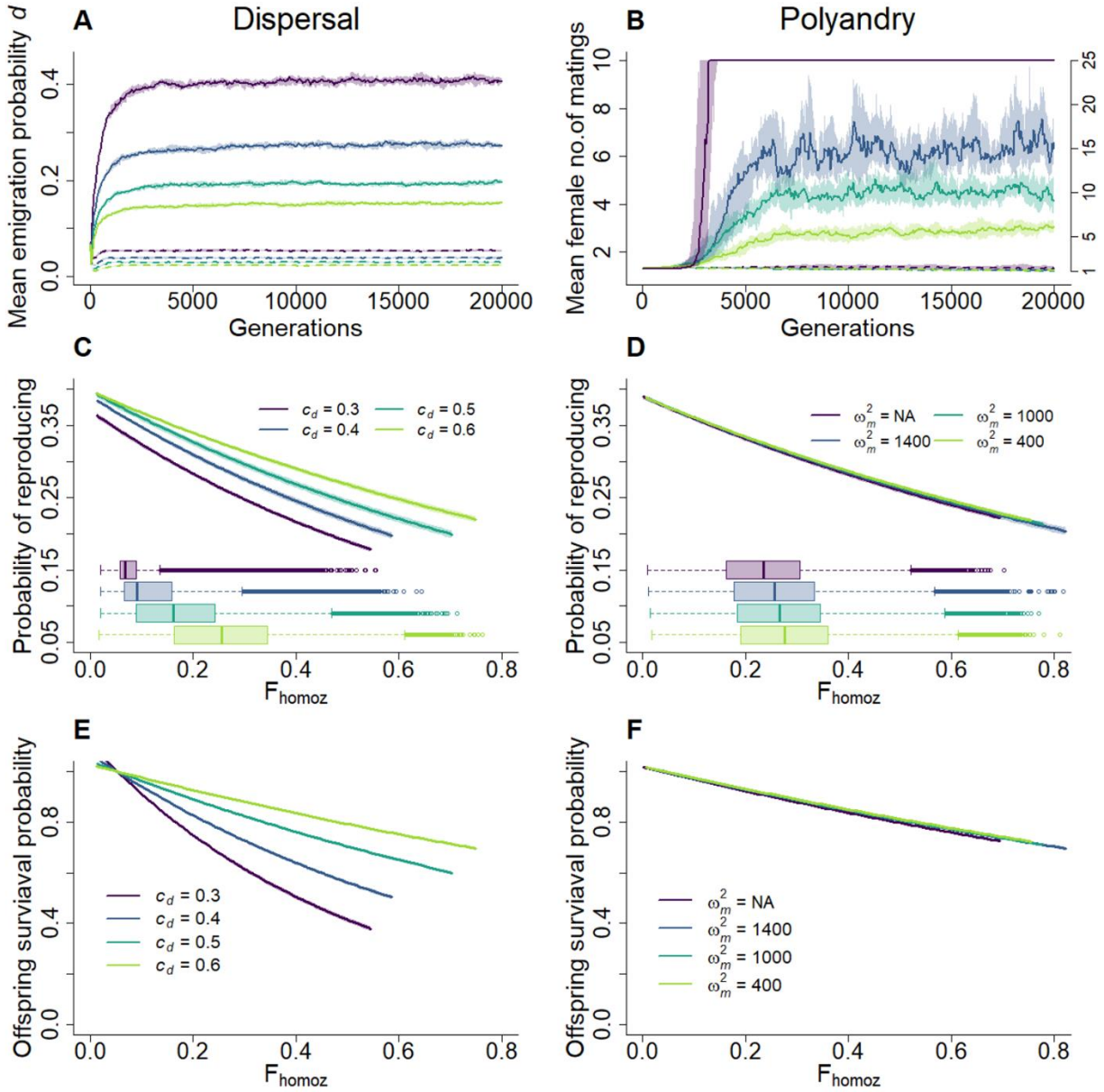

Figure 1. Inbreeding depression promotes evolution of dispersal and polyandry when either one trait or the other evolves. A) Evolution of mean dispersal probability phenotypes *d* in the absence of polyandry (*a* = 3.0), under different costs of dispersal (c_d = 0.3, 0.4, 0.5, 0.6), in the absence (dashed lines) or presence (solid lines) of deleterious mutations. **B)** Evolution of mean polyandry phenotypes (expected female number of matings *P* = 1 + 1/*a*) under fix dispersal probability (*d* = 0.05), as a function of different strengths of direct selection against female remating (no cost; ω_m^2 = 1400, 1000, 400) in the absence (dashed lines) or presence (solid lines) of deleterious mutations. In the presence of deleterious mutations and no direct selection against

polyandry (ω_m^2= NA), females evolve to mate with all the males in the population; the y-axis on the right hand-side refers to this single line (purple). Lines represent the median of mean phenotypes across 20 replicated simulations; colored shades depict the first and third quartile. **C-D)** Relationship between individual probability of reproducing and inbreeding coefficient F_{homoz} (i.e., ID in reproduction probability) when C) dispersal evolves under different costs, in the absence of polyandry and, D) polyandry evolves under different strengths of direct selection, with fix dispersal probability. Lines show the fitted models and colored shades the 95% CI. Models are fitted at generation 20,000 to a subsample of 140 populations, across 10 replicates. Boxplots represents the distribution of the individual F_{homoz}. **E-F)** Relationship between offspring survival probability and F_{homoz} (i.e., ID in offspring survival probability). In E) simulation scenarios and parameters as in C); in F) as in D). The coefficients (i.e., mutation load and inbreeding load) and standard errors of all the fitted models are presented in Table S2.

These results provide a positive answer to the still standing question of whether costly polyandry can evolve, at least in theory, as a mechanism of indirect inbreeding avoidance in spatially structured populations (Germain et al. 2018). Specifically, they show that costly polyandry, although the cost needs to be quite low, as predicted by (Cornell and Tregenza 2007), can indeed evolve in response to inbreeding depression given: i) inbreeding depression caused exclusively by deleterious recessive mutations, and without the need for overdominant mutations (Cornell and Tregenza 2007); ii) realistic deleterious mutation rates and distribution of fitness effects (Caballero and Keightley 1994; Schultz and Lynch 1997; Haag-Liautard et al. 2007); iii) and complex sibship structure emerging in spatially structured populations (Germain et al. 2018). Thus, polyandry evolution as a means of indirect inbreeding avoidance might be more widely spread than previously thought (Cornell and Tregenza 2007; Germain et al. 2018), and therefore a potentially important mechanism to explain the existence of even low levels of polyandry across multiple systems, especially when dispersal is low.

Although polyandry evolved in response to the presence of genetic load, the level of evolved polyandry under different costs did not substantially change the level of inbreeding (measured as neutral homozygosity) and ID at equilibrium (Fig. 1D-F; Table S2; Fig. S1D-F; S2D-

F). In fact, both the mutation load and ID were the same across levels of evolved polyandry and polyandry's costs. The level of mutation and inbreeding load was mainly determined by dispersal, which was fixed to d = 0.05, and similar to what evolved under high cost of dispersal and no polyandry (Fig. 1C-E). This was true also for heterosis (Fig. S4). Thus, under low fixed dispersal probability, polyandry seems to have a minimal effect, if any, on the purging or accumulation of genetic load, ID and, not surprisingly, heterosis. Unlike with dispersal therefore, with polyandry there seems not to be scope for a positive feedback with inbreeding depression, but just for one-direction effect of inbreeding depression on polyandry evolution.

***Joint evolution of dispersal, polyandry, and inbreeding depression*.** When dispersal and polyandry could evolve jointly, results clearly confirmed the hypothesis of a negative feedback between two competing mechanisms of inbreeding avoidance (Fig. 2; S5). This feedback was modulated by the relative costs of the two evolving behaviors. For a given cost of dispersal (c_d), higher dispersal evolved under monandry; *vice versa*, the higher the evolved level of polyandry (hence for lower costs of female re-mating) the lower the evolved emigration probability. For example, c_d = 0.3 led to evolution of median $\bar{d}$ = 0.39 (95%CI 0.375-0.396) and median $\overline{P}$ = 1.97 (95%CI 1.763-2.173) for high cost of female re-mating (ω_m^2= 400), while it led to median $\bar{d}$ = 0.31 (95%CI 0.312-0.322) and to females mating with all the males in the population (P = 25) when female re-mating did not carry costs. On the other hand, for a given cost of female re-mating, higher polyandry evolved given lower evolved dispersal (hence for higher c_d). For example, ω_m^2= 1000 led to evolution of median $\bar{d}$ = 0.13 (95%CI 0.126-0.131) and median $\overline{P}$ = 4.49 (95%CI 3.842-5.317) for high cost of dispersal (c_d = 0.6), while it led to median $\bar{d}$ = 0.38 (95%CI 0.36-0.383) and median $\overline{P}$ = 2.58 (95%CI 2.467-2.814) for c_d = 0.3. This joint evolution and negative feedback did not emerge when the two traits evolved in the absence of genetic load and hence ID (Fig. S6), where dispersal evolved to very low levels while polyandry did not evolve.

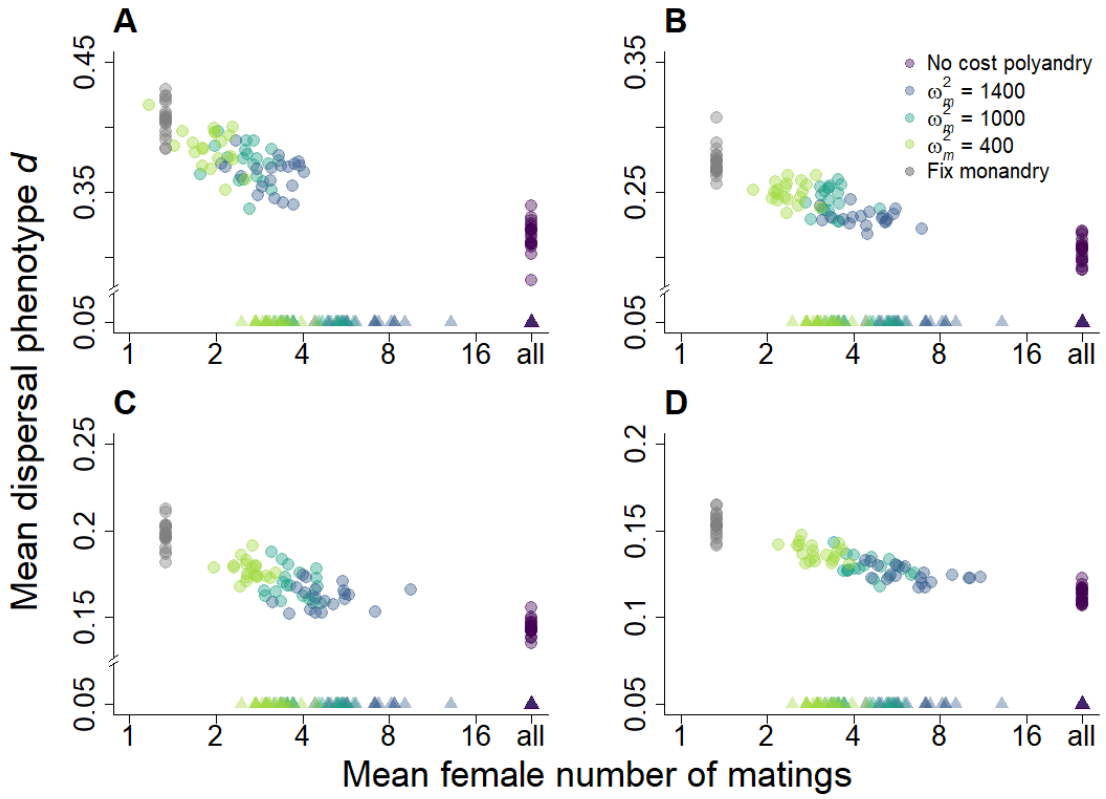

388

389 **Figure 2. Dispersal and polyandry negatively feedback to each other evolution under**
390 **inbreeding depression.** Joint evolution of mean dispersal probability phenotypes *d* and mean
391 polyandry phenotypes (mean female number of matings: $P = 1 + 1/a$) in the presence of
392 inbreeding depression, given different costs of dispersal c_d (**A:** 0.3; **B:** 0.4; **C:** 0.5; **D:** 0.6) and
393 different strengths of direct selection against female re-mating (no cost; ω_m^2= 1400, 1000, 400).
394 Each data point represents the mean phenotypic values for one out of 20 replicate simulations at
395 generation 20,000. Colored dots indicate simulations where dispersal and polyandry jointly
396 evolved; triangles, simulations where polyandry evolved given fix dispersal probability (d = 0.05);
397 grey dots, simulations where dispersal evolved given fix monandry (a = 3.0). The x-axis is on the
398 logarithmic scale to aid visualization. Note the different y-axis scales for the four panels. Other
399 parameters: U_d = 1.0, U_l = 0.2.

400

401 The negative correlation between evolved emigration probability (d) and polyandry (P)
402 was present at the metapopulation level (i.e., simulation replicate level), whereby for a given cost
403 of dispersal and strength of direct selection on female re-mating, systems that evolved higher

404 emigration probability phenotypes, also evolved lower polyandry, and *vice versa* (Fig. S7). This
405 correlation was present when female re-mating was costly; in the absence of re-mating costs the
406 correlation disappeared as females consistently evolved to mate with all the males in the
407 population. Within a metapopulation, there was no evidence of a negative correlation between *d*
408 and *P*, whereby subpopulations with higher dispersal might have had lower polyandry (Fig. S8).
409 Further, there was no evidence of any genetic correlation between g_d and g_a, nor between *d* and
410 *P* (Fig. S9).

411 Lower rates of mildly deleterious and lethal mutations led to evolution of lower dispersal
412 and polyandry (Fig. S10), similarly to when the two traits evolved independently (Fig. S1-S2).
413 Polyandry hardly evolved, apart from a few exception simulations under no or weak direct
414 selection against female re-mating, where it reached high levels. A strong negative correlation
415 between dispersal and polyandry phenotypes was present at the metapopulation level when some
416 polyandry evolved, while it disappeared for very low mutation rates combined with costly
417 polyandry (Fig. S11). As for higher rates of deleterious mutations, at lower mutation rates there
418 was no evidence of a negative correlation between dispersal and polyandry at the subpopulation
419 level, nor of any genetic correlation (Fig. S12-S13).

420 The evolved level of ID depended mainly on the cost of dispersal, and hence on the level
421 of evolved dispersal (Fig. 3-4; Table S3). As for the scenario where dispersal evolved under fixed
422 monandry (Fig. 1C-E), higher cost and consequent lower evolved dispersal led to lower
423 inbreeding depression to both probability of reproducing (Fig. 3A, Fig. 4 diamonds) and offspring
424 survival (Fig. 3B, Fig. 4 dots). Interestingly, under the joint evolution of dispersal and polyandry,
425 polyandry had a slight but detectable effect on the level of evolved ID, compared to when evolving
426 under fixed low dispersal (Fig. 1D-F). Specifically, for a given dispersal cost, higher polyandry
427 (lower strength of direct selection on female re-mating) led to the accumulation of lower inbreeding

428 load in offspring survival, especially for lower costs of dispersal (Fig. 4 dots; Table S3). The
429 difference was especially evident when comparing no cost *vs* costly polyandry. For the inbreeding
430 load in adult reproduction, this effect was present but only very slight and with overlapping
431 confidence intervals between different costs of polyandry (Fig. 4 diamonds; Table S3). This result
432 is perhaps surprising and counterintuitive as the expectation would be for more polyandry to lead
433 to accumulation of higher load, due to reduced inbreeding and purging, and not the opposite as
434 observed here. However, this effect might be due to high polyandry reducing evolved dispersal
435 thus, in fact, facilitating slightly greater purging through its effect on dispersal.

436 Finally, the emerging heterosis in the system was exclusively driven by the level of evolved
437 dispersal, and hence by dispersal cost. Higher heterosis was present under high costs of
438 dispersal, thus generating strong positive selection for dispersal, counteracting the high cost (Fig.
439 4B).

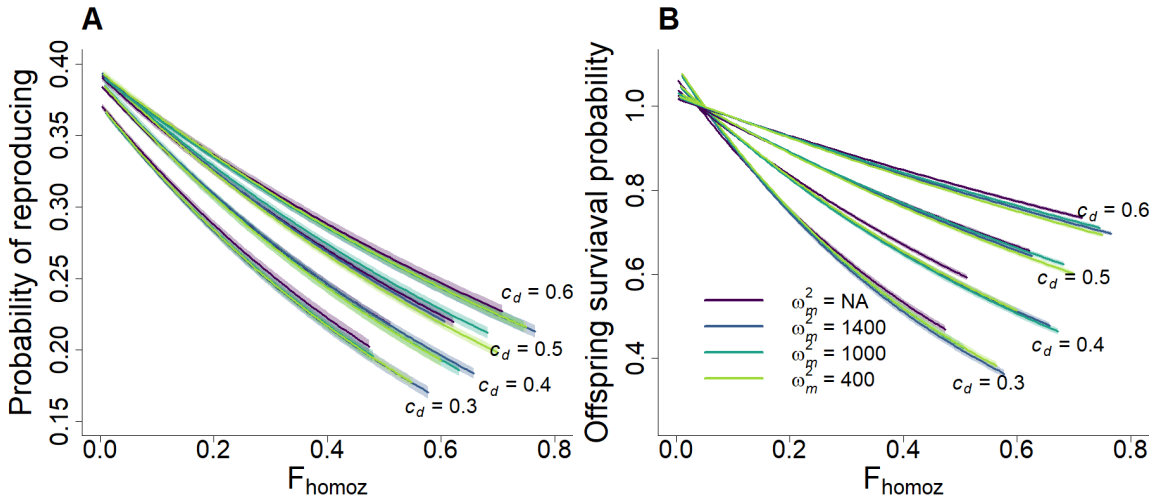

440

441

442 **Figure 3. Jointly evolving dispersal and polyandry affect evolution of inbreeding**
443 **depression in reproduction and survival.** Relationship between **A)** individual probability of
444 reproducing and neutral homozygosity F_{homoz} (i.e., inbreeding depression in reproduction
445 probability), and **B)** between offspring survival probability and neutral homozygosity (i.e.,

inbreeding depression in offspring survival probability). Results are presented for varying costs of dispersal (c_d) and strengths of direct selection against female multiple mating (ω_m^2; colors). Lines show the fitted models and colored shades the 95% CI. The coefficients (i.e., mutation load and inbreeding load) and standard errors of all the fitted models are presented in Table S3. Models are fitted at generation 20,000 to a subsample of 140 populations, across 10 replicates.

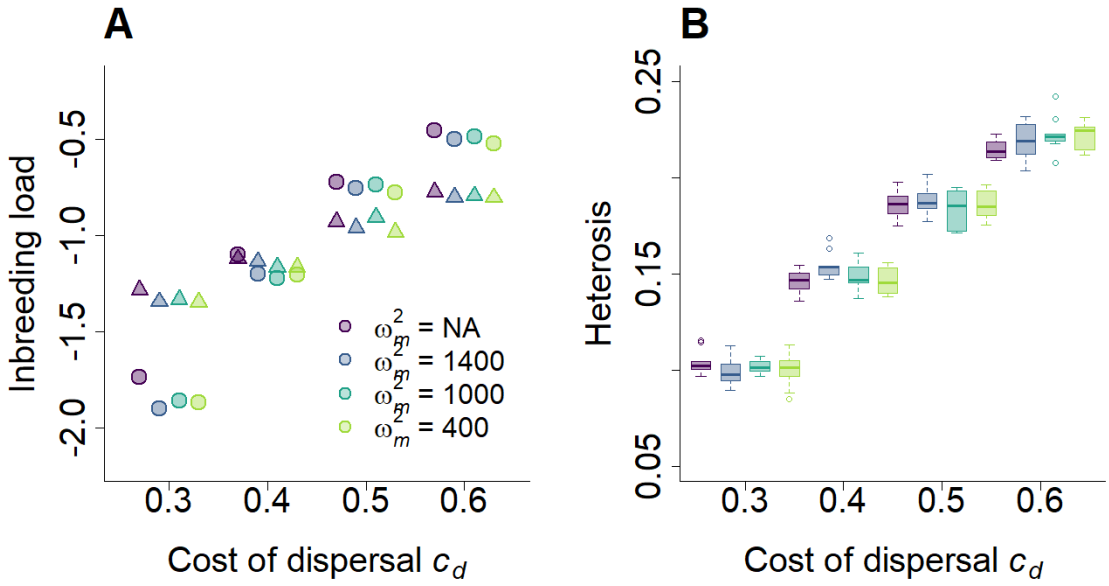

Figure 4. Inbreeding load and heterosis emerging under the joint evolution of dispersal and polyandry. A) Estimated slopes of probability of offspring survival (dots) and probability of reproduction (triangles) on individual neutral homozygosity F_{homoz} (i.e., inbreeding load), for different cost of dispersal (c_d) and strengths of direct selection on female multiple mating (ω_m^2; colors). Results are presented on the log scale. Standard errors are not shown because smaller than the dots size. Models are fitted at generation 20,000 to a subsample of 140 populations, across 10 replicates. **B)** Heterosis as a function of c_d and ω_m^2 (the color legend is the same as in A). Heterosis is shown as median (solid bands), first and third quartiles (box limits), and approximately twice the standard deviation (whiskers) over 20 replicate simulations at generation 20,000.

***General discussion*.** These results shed light on the previously unconsidered intimate connection existing between dispersal and polyandry evolution through their shared driver of inbreeding depression, and on their effect on evolution of inbreeding depression itself. They highlight important interactions between the evolution of two fundamental life-histories which shape gene flow in space and time, and thereby affect species' eco-evolutionary dynamics. More broadly, these results demonstrate the need to consider life-history evolution as happening within a complex and integrated system, where multiple competing and degenerate routes to reduce fitness costs can arise and affect each other's evolutionary dynamics (Edelman and Gally 2001; Mason 2015). This becoming strongly apparent in different complex biological systems, such as genetic codes and networks, neural networks, organismal development, population and community dynamics (see examples within Edelman and Gally 2001; Mason 2015)), but perhaps it has not been into the investigation of life-history evolution. For example, within the context of evolution of polyandry as inbreeding avoidance strategy, Duthie et al. (2018) showed that evolution of pre-copulatory and post-copulatory mechanisms of inbreeding avoidance and associated polyandry is affected by evolutionary feedbacks and degeneracy. Thus, understanding when and how we can expect to observe different patterns of life-history traits co-occurrence requires explicitly modelling feedbacks between competing and / or complementary evolutionary routes.

Here, I show that through their effect on the population relatedness structure, and hence on inbreeding levels, dispersal and polyandry can negatively feedback to each other evolution, thereby providing two competing mechanisms for compensating the negative fitness effects of genetic load. The engine of this feedback is inbreeding depression. Without genetic load giving rise to inbreeding depression and heterosis, kin competition alone is not sufficient for a negative relationship between dispersal and polyandry to emerge, nor for polyandry to evolve. Despite the

recognition that dispersal and mating system evolution may be profoundly interconnected, leading to observable dispersal-mating system syndromes (Ronce and Clobert 2012; Auld and Rubio de Casas 2013; Hargreaves and Eckert 2014), previous theory has rarely focused on their joint evolution, with the notable exception of joint evolution of dispersal and self-fertilization (Massol and Cheptou 2011; Sun and Cheptou 2012; Iritani and Cheptou 2017). Further, the relatively recent recognition of the widespread occurrence and importance of female multiple mating meant that the relationship of this key component of many mating systems with dispersal has been understudied compared to monogamy and polygyny. Probably the paucity of theory and clear testable predictions, and the inherent difficulties in studying these two complex suits of behaviors empirically (Rhainds 2017), underlie the scarcity of empirical evidence on patterns of dispersal-polyandry co-occurrence and joint evolution, especially, but not exclusively, at the individual level (Laloi et al. 2009; Reid and Arcese 2020).

This model provides the clear prediction of a negative correlation between dispersal and female multiple mating at the species or metapopulation level, provided the presence of inbreeding depression. This means that we might expect to find that females of highly dispersive species (or metapopulations) engage less in multiple mating, while expecting to observe high frequency of female multiple mating in highly philopatric species (or metapopulations) for which, for example, dispersal is very costly. A recent analysis of song sparrow's (*Melospiza melodia*) long term pedigree data from the population occupying the small island of Mandarte (British Columbia, Canada) showed that recent immigrants to the population had lower breeding values for female extra-pair reproduction (which results from underlying polyandry) than the local population (Reid and Arcese 2020). This rare empirical evidence points towards a negative correlation between dispersal and female multiple mating, in this case present between the island

512 and the mainland (much larger) population, although the causes of such relationship are currently
513 unknown.

514 Results from my current model did not show any covariance between polyandry and
515 dispersal at finer spatial scale (e.g., within a metapopulation), or at the individual level. Likewise,
516 very few empirical studies have explicitly tested for the presence of such covariance, and not
517 always found evidence of it (Rhainds 2017; Rafter et al. 2018; Reid and Arcese 2020). However,
518 there are assumptions embedded within the model structure that could affect these predictions,
519 pointing towards the need for further theoretical work needed to resolve whether we should expect
520 any covariance between these two traits at the population or individual level. The model is
521 ecologically quite simple; the environment is spatially homogeneous as are the costs of dispersal
522 and polyandry. Similarly, the relatively high levels of dispersal evolving, combined with the long-
523 distance dispersal allowed by the negative exponential dispersal kernel and the homogeneous
524 environment (and consequently homogeneous risk of inbreeding), impede populations to diverge
525 in their evolutionary trajectories for dispersal and polyandry, such that populations evolve as a
526 single system despite the emerging internal relatedness structure. A spatially heterogeneous
527 environment where, for example, some populations are more isolated than others, or where
528 populations experience different costs of dispersal and/or polyandry, may promote a negative
529 relationship between dispersal and polyandry at the population level whereby frequency of female
530 multiple mating may be expected to be higher in more isolated populations.

531 The model does not allow for evolution of sex-biased dispersal (Li and Kokko 2019).
532 Although evolution of sex-biased dispersal is not a necessary condition for inbreeding avoidance
533 through dispersal (Guillaume and Perrin 2009; Roze and Rousset 2009; Li and Kokko 2019)and,
534 on the other hand, it is itself affected by multiple ecological and evolutionary drivers other than
535 inbreeding depression (Henry et al. 2016; Li and Kokko 2019), evolution of sex-biased dispersal

could change the dynamics of joint evolution of dispersal and polyandry in ways that are difficult to predict without explicit investigation. Evolution of sex-biased dispersal and the direction of the bias depend on sex differences in fitness variance between patches, where, generally, the sex with the larger between-patch variance in fitness evolves to disperse more (Li and Kokko 2019). As the effect of polyandry on sex-specific variance in fitness is hard to predict (Lotterhos 2011; Bocedi and Reid 2017), this cascades in the challenge to predict its effect on sex-biased dispersal. Interestingly, although previous models considered the effect of different mating systems on the evolution of sex-biased dispersal given inbreeding depression (Hirota 2005; Guillaume and Perrin 2009; Henry et al. 2016), no model to my knowledge has considered the opposite, that is the effect of sex-biased dispersal on mating system evolution, nor the potential feedbacks between the two, revealing yet another knowledge gap in our understanding of life-history evolution in spatially structured systems.

The life cycle represented in this model is also relatively simplified with mating occurring after dispersal and non-overlapping generations. The timing of mating relative to dispersal can affect gene flow and the genetic structure of the population thereby affecting evolution of both dispersal and mating system (Hirota 2004; Shaw and Kokko 2015; Lakovic et al. 2017). In species with post-mating dispersal, as many invertebrate species where females disperse after mating and before oviposition, polyandry has been hypothesized to be particularly beneficial for dispersing females colonizing new habitat patches as their offspring would benefit from half-sib rather than full-sib matings, thus reducing the level of inbreeding in the females' grand-offspring (Cornell and Tregenza 2007). Moreover, post-mating dispersal is much less effective, if at all, in avoiding inbreeding as mating takes place within the natal population (Li and Kokko 2019). In this case, a positive covariance between dispersal and polyandry would be expected. Although high levels of polyandry have been demonstrated in the field for two stored grain pest beetles with

post-mating dispersal, a positive covariance between dispersal and female multiple mating has not been found (Rafter et al. 2018). This positive association between polyandry and dispersal in species with post-mating dispersal could be particularly beneficial during colonization of empty patches thus, for example during range expansion or shifting, relative to within an established spatially structured population (Rafajlović et al. 2013; Ding et al. 2017). Indeed, experimental studies with seed and flour beetles have shown that multiple mated females establish fitter populations both in benign and thermally challenging environments (Power and Holman 2014; Lewis et al. 2020). These results, together with the ones presented here, point to the possibility that the relationship between dispersal and polyandry will be dependent on the ecological and demographic context, and on other species' life-histories. However, we lack theoretical predictions on how dispersal and polyandry may covary under range expansion conditions, under different timing of dispersal relative to mating, as well as we lack empirical estimates of such covariance under both static and dynamic spatial structure. There is therefore large and interesting potential to step-up and expand our knowledge on the evolution of dispersal and mating systems by embracing their joint evolution and feedbacks, theoretically as well as empirically.

Acknowledgments

I am grateful to J. M. Reid and J. M. J. Travis as this work would not have been possible without their mentorship. I thank A. B. Duthie, M. Tschol, A. Charmouh and L. Dunan for helpful discussions. This work was supported by a Royal Society University Research Fellowship to GB (UF160614), and initially by the European Research Council through funding to J.M. Reid. All simulations were performed on the University of Aberdeen HPC, Maxwell.

References

Agrawal, A. F., and M. C. Whitlock. 2011. Inferences about the distribution of dominance drawn from yeast gene knockout data. Genetics 187:553–566.

Arnqvist, G., and T. Nilsson. 2000. The evolution of polyandry: multiple mating and female fitness in insects. Anim Behav 60:145–164.

Auld, J. R., and R. Rubio de Casas. 2013. The Correlated Evolution of Dispersal and Mating-System Traits. Evol Biol 40:185–193.

Bocedi, G., and J. M. Reid. 2017. Feed-backs among inbreeding, inbreeding depression in sperm traits, and sperm competition can drive evolution of costly polyandry. Evolution 71:2786–2802.

Caballero, A., and P. D. Keightley. 1994. A pleiotropic nonadditive model of variation in quantitative traits. Genetics 138:883–900.

Charlesworth, D., and B. Charlesworth. 1987. Inbreeding depression and its evolutionary consequences. Annu Rev Ecol Syst 18:237–268.

Charlesworth, D., and J. H. Willis. 2009. The genetics of inbreeding depression. Nat Rev Genet 10:783–96.

Cheptou, P., A. Hargreaves, D. Bonte, and H. Jacquemyn. 2017. Adaptation to fragmentation: Evolutionary dynamics driven by human influences. Philosophical Transactions of the Royal Society B 372:20160037.

Clobert, J., M. Baguette, T. G. Benton, and J. M. Bullock. 2012. Dispersal Ecology and Evolution. Oxford University Press.

Cornell, S. J., and T. Tregenza. 2007. A new theory for the evolution of polyandry as a means of inbreeding avoidance. Proceedings of the Royal Society B 274:2873–9.

Ding, G., H. Xu, B. P. Oldroyd, and R. S. Gloag. 2017. Extreme polyandry aids the establishment of invasive populations of a social insect. Heredity 119:381–387.

Duthie, A. B., G. Bocedi, R. R. Germain, and J. M. Reid. 2018. Evolution of precopulatory and post-copulatory strategies of inbreeding avoidance and associated polyandry. J Evol Biol 31:31–45.

Duthie, A. B., G. Bocedi, and J. M. Reid. 2016. When does female multiple mating evolve to adjust inbreeding? Effects of inbreeding depression, direct costs, mating constraints, and polyandry as a threshold trait. Evolution 70:1927–1943.

Edelman, G. M., and J. A. Gally. 2001. Degeneracy and complexity in biological systems. Proceedings of the National Academy of Sciences 98:13763–13768.

Eyre-Walker, A., and P. D. Keightley. 2007. The distribution of fitness effects of new mutations. Nat Rev Genet 8:610–8.

Fromhage, L., H. Kokko, and J. M. Reid. 2009. Evolution of mate choice for genome-wide heterozygosity. Evolution 63:684–94.

621 Gandon, S. 1999. Kin competition, the cost of inbreeding and the evolution of dispersal. J Theor
622 Biol 200:345–364.

623 Germain, R. R., P. Arcese, and J. M. Reid. 2018. The Consequences of Polyandry for Sibship
624 Structures, Distributions of Relationships and Relatedness, and Potential for Inbreeding in
625 a Wild Population. Am Nat 191:638–657.

626 Gilbert, K. J., N. P. Sharp, A. L. Angert, G. L. Conte, J. A. Draghi, F. Guillaume, A. L.
627 Hargreaves, R. Matthey-Doret, and M. C. Whitlock. 2017. Local Adaptation Interacts with
628 Expansion Load during Range Expansion: Maladaptation Reduces Expansion Load. Am
629 Nat 189:368–380.

630 Guillaume, F., and N. Perrin. 2009. Inbreeding load, bet hedging, and the evolution of sex-
631 biased dispersal. Am Nat 173:536–41.

632 Guillaume, F., and N. Perrin. 2006. Joint evolution of dispersal and inbreeding load. Genetics
633 173:497–509.

634 Haag-Liautard, C., M. Dorris, X. Maside, S. Macaskill, D. L. Halligan, D. Houle, B. Charlesworth,
635 and P. D. Keightley. 2007. Direct estimation of per nucleotide and genomic deleterious
636 mutation rates in *Drosophila*. Nature 445:82–85.

637 Hanski, I. 2011. Eco-evolutionary spatial dynamics in the Glanville fritillary butterfly. Proc Natl
638 Acad Sci USA 108:14397–14404.

639 Hargreaves, A. L., and C. G. Eckert. 2014. Evolution of dispersal and mating systems along
640 geographic gradients: Implications for shifting ranges. Funct Ecol 28:5–21.

641 Hedrick, P. W., and A. Garcia-Dorado. 2016. Understanding Inbreeding Depression, Purging,
642 and Genetic Rescue. Trends Ecol Evol 31:940–952. Elsevier Ltd.

643 Henry, R. C., A. Coulon, and J. M. J. Travis. 2016. The evolution of male-biased dispersal under
644 the joint selective forces of inbreeding load and demographic and environmental
645 stochasticity. Am Nat 188:423–433.

646 Hirota, T. 2005. The effect of female polyandry and sperm precedence on the evolution of
647 sexual difference in dispersal timing. J Evol Biol 1395–402.

648 Hirota, T. 2004. The evolution of sex-biased dispersal by pre-dispersal copulation and
649 fluctuating environment. J Anim Ecol 73:1115–1120.

650 Holman, L., and H. Kokko. 2013. The consequences of polyandry for population viability,
651 extinction risk and conservation. Philosophical Transactions of the Royal Society B
652 368:20120053.

653 Huber, C. D., A. Durvasula, A. M. Hancock, and K. E. Lohmueller. 2018. Gene expression
654 drives the evolution of dominance. Nat Commun 9.

655 Iritani, R., and P. O. Cheptou. 2017. Joint evolution of differential seed dispersal and self-
656 fertilization. J Evol Biol 30:1526–1543.

Jennions, M. D., and M. Petrie. 2000. Why do females mate multiply? A review of the genetic benefits. Biological Reviews 75:21–64.

Keller, L., and D. Waller. 2002. Inbreeding effects in wild populations. Trends Ecol Evol 17:19–23.

Kimura, M. 1965. A stochastic model concerning the maintenance of genetic variability in quantitative characters. Proc Natl Acad Sci USA 54:731–736.

Kvarnemo, C., and L. Simmons. 2013. Polyandry as a mediator of sexual selection before and after mating. Philosophical Transactions of the Royal Society B 368:20120042.

Lakovic, M., O. Mitesser, and T. Hovestadt. 2017. Mating timing, dispersal and local adaptation in patchy environments. Oikos 126:1804–1814.

Laloi, D., M. Richard, P. Fédérici, J. Clobert, P. Teillac-Deschamps, and M. Massot. 2009. Relationship between female mating strategy, litter success and offspring dispersal. Ecol Lett 12:823–9.

Lande, R., and D. Schemske. 1985. The evolution of self-fertilization and inbreeding depression in plants. I. Genetic models. Evolution 39:24–40.

Lande, R., D. W. Schemske, and S. T. Schultz. 1994. High inbreeding depression, selective interference among loci, and the threshold selfing rate for purging recessive lethal mutations. Evolution 48:965–978.

Legrand, D., J. Cote, E. A. Fronhofer, R. D. Holt, O. Ronce, N. Schtickzelle, J. M. J. Travis, and J. Clobert. 2017. Eco-evolutionary dynamics in fragmented landscapes. Ecography 40:9–25.

Lewis, R. C., M. D. Pointer, L. A. Friend, R. Vasudeva, J. Bemrose, A. Sutter, M. J. G. Gage, and L. G. Spurgin. 2020. Polyandry provides reproductive and genetic benefits in colonising populations. Ecol Evol 10:10851–10857.

Li, X. Y., and H. Kokko. 2019. Sex-biased dispersal: a review of the theory. Biological Reviews 94:721–736.

Lotterhos, K. E. 2011. The context-dependent effect of multiple paternity on effective population size. Evolution 65:1693–1706.

Markert, J. A., P. R. Grant, B. R. Grant, L. F. Keller, J. L. Coombs, and K. Petren. 2004. Neutral locus heterozygosity, inbreeding, and survival in Darwin's ground finches (*Geospiza fortis* and *G. scandens*). Heredity 92:306–315.

Mason, P. H. 2015. Degeneracy: Demystifying and destigmatizing a core concept in systems biology. Complexity 20:12–21.

Massol, F., and P. O. Cheptou. 2011. When should we expect the evolutionary association of self-fertilization and dispersal? Evolution 65:1217–1220.

Morton, N. E., J. F. Crow, and H. J. Muller. 1956. An estimate of the mutational damage in man from data on consanguineous marriages. Proc Natl Acad Sci U S A 42:855–863.

694 Neff, B. D., and T. E. Pitcher. 2008. Mate choice for non-additive genetic benefits: a resolution
695 to the lek paradox. J Theor Biol 254:147–55.

696 Nietlisbach, P., S. Muff, J. M. Reid, M. C. Whitlock, and L. F. Keller. 2019. Nonequivalent lethal
697 equivalents: Models and inbreeding metrics for unbiased estimation of inbreeding load.
698 Evol Appl 12:266–279.

699 Parker, G., and T. Birkhead. 2013. Polyandry: the history of a revolution. Philosophical
700 Transactions of the Royal Society B 368:20120335.

701 Peischl, S., M. Kirkpatrick, and L. Excoffier. 2015. Expansion Load and the Evolutionary
702 Dynamics of a Species Range. Am Nat 185:E81–E93.

703 Perrin, N., and J. Goudet. 2001. Inbreeding, kinship, and the evolution of natal dispersal. Pp.
704 123–142 *in* J. Clobert, E. Danchin, A. A. Dhondt, and J. D. Nichols, eds. Dispersal. Oxford
705 University Press, Oxford.

706 Perrin, N., and V. Mazalov. 1999. Dispersal and inbreeding avoidance. Am Nat 154:282–292.

707 Perrin, N., and V. Mazalov. 2000. Local competition, inbreeding, and the evolution of sex-biased
708 dispersal. Am Nat 155:116–127.

709 Pike, V. L., C. K. Cornwallis, and A. S. Griffin. 2021. Why don't all animals avoid inbreeding?
710 Proceedings of the Royal Society B 288:20211045.

711 Pizzari, T., and N. Wedell. 2013. The polyandry revolution. Philosophical Transactions of the
712 Royal Society B 368:20120041.

713 Porcher, E., and R. Lande. 2016. Inbreeding depression under mixed outcrossing, self-
714 fertilization and sib-mating. BMC Evol Biol 16:105.

715 Porcher, E., and R. Lande. 2005. Loss of gametophytic self-incompatibility with evolution of
716 inbreeding depression. Evolution 59:46–60.

717 Power, D. J., and L. Holman. 2014. Polyandrous females found fitter populations. J Evol Biol
718 27:1948–1955.

719 R Core Team. 2019. R: A Language and Environment for Statistical Computing. R Foundation
720 for Statistical Computing, Vienna, Austria.

721 Rafajlović, M., A. Eriksson, A. Rimark, S. Hintz-Saltin, G. Charrier, M. Panova, C. André, K.
722 Johannesson, and B. Mehlig. 2013. The Effect of Multiple Paternity on Genetic Diversity of
723 Small Populations during and after Colonisation. PLoS One 8:1–9.

724 Rafter, M. A., G. A. McCulloch, G. J. Daglish, K. Gurdasani, and G. H. Walter. 2018. Polyandry,
725 genetic diversity and fecundity of emigrating beetles: understanding new foci of infestation
726 and selection. J Pest Sci (2004) 91:287–298.

727 Ravigné, V., I. Olivieri, S. Gonzalez-Martinez, and F. Roussett. 2006. Selective Interactions
728 Between Short-Distance Pollen and Seed Dispersal in Self-Compatible Species. Evolution
729 60:2257–2271.

730 Reid, J. M., and P. Arcese. 2020. Recent immigrants alter the quantitative genetic architecture
731 of paternity in song sparrows. Evol Lett 4:124–136.

732 Reid, J. M., P. Arcese, L. F. Keller, R. R. Germain, A. B. Duthie, S. Losdat, M. E. Wolak, and P.
733 Nietlisbach. 2015. Quantifying inbreeding avoidance through extra-pair reproduction.
734 Evolution 69:59–74.

735 Reid, J. M., and R. J. Sardell. 2012. Indirect selection on female extra-pair reproduction?
736 Comparing the additive genetic value of maternal half-sib extra-pair and within-pair
737 offspring. Proceedings of the Royal Society B 279:1700–8.

738 Rhainds, M. 2017. Polyandry across Behavioral Classes in Female Spruce Budworm. J Insect
739 Behav 30:662–673.

740 Ronce, O. 2007. How Does It Feel to Be Like a Rolling Stone? Ten Questions About Dispersal
741 Evolution. Annu Rev Ecol Evol Syst 38:231–253.

742 Ronce, O., and J. Clobert. 2012. Dispersal syndrome. P. *in* J. Clobert, M. Baguette, T. G.
743 Benton, and J. M. Bullock, eds. Dispersal Ecology and Evolution. Oxford University Press.

744 Roze, D., and F. Rousset. 2009. Strong effects of heterosis on the evolution of dispersal rates. J
745 Evol Biol 22:1221–1233.

746 Schultz, S. T., and M. Lynch. 1997. Mutation and Extinction: The Role of Variable Mutational
747 Effects, Synergistic Epistasis, Beneficial Mutations, and Degree of Outcrossing. Evolution
748 51:1363–1371.

749 Shaw, A. K., and H. Kokko. 2015. Dispersal evolution in the presence of Allee effects can speed
750 up or slow down invasions. Am Nat 185:631–639.

751 Simmons, M. J., and J. F. Crow. 1977. Mutations affecting fitness in Drosophila populations.
752 Annu Rev Genet 11:49–78.

753 Slatyer, R. A., B. S. Mautz, P. R. Y. Backwell, and M. D. Jennions. 2012. Estimating genetic
754 benefits of polyandry from experimental studies: a meta-analysis. Biological Reviews 87:1–
755 33.

756 Spigler, R. B., K. Theodorou, and S.-M. Chang. 2017. Inbreeding depression and drift load in
757 small populations at demographic disequilibrium. Evolution 71:81–94.

758 Stockley, P., J. B. Searle, D. W. MacDonald, and C. S. Jones. 1993. Female multiple mating
759 behaviour in the common shrew as a strategy to reduce inbreeding. Proceedings of the
760 Royal Society B 254:173–9.

761 Sun, S., and P. Cheptou. 2012. Life-history traits evolution across distribution ranges: how the
762 joint evolution of dispersal and mating system favor the evolutionary stability of range
763 limits? Evol Ecol 26:771–778.

764 Szulkin, M., and B. C. Sheldon. 2008. Dispersal as a means of inbreeding avoidance in a wild
765 bird population. Proceedings of the Royal Society B: Biological Sciences 275:703–11.

766 Szulkin, M., K. Stopher, J. Pemberton, and J. Reid. 2013. Inbreeding avoidance, tolerance, or
767 preference in animals? Trends Ecol Evol 28:205–211.

768 Taylor, M. L., T. A. R. Price, and N. Wedell. 2014. Polyandry in nature: a global analysis. Trends
769 Ecol Evol 29:376–83.

770 Theodorou, K., and D. Couvet. 2006. On the expected relationship between inbreeding, fitness,
771 and extinction. Genetics Selection Evolution 38:371–387.

772 Tregenza, T., and N. Wedell. 2002. Polyandrous females avoid costs of inbreeding. Nature
773 415:71–73.

774 Waser, P., S. Austad, and B. Keane. 1986. When should animals tolerate inbreeding? Am Nat
775 128:529–537.

776 Whitlock, M. C., P. K. Ingvarsson, and T. Hatfield. 2000. Local drift load and the heterosis of
777 interconnected populations. Heredity 84:452–457.

778 Zhu, Y. O., M. L. Siegal, D. W. Hall, and D. a Petrov. 2014. Precise estimates of mutation rate
779 and spectrum in yeast. Proceedings of the National Academy of Sciences 111:E2310–
780 E2318.

781

782

Inbreeding depression drives evolution of dispersal and polyandry

Supplementary Material

Greta Bocedi[1]

[1]School of Biological Sciences, University of Aberdeen, Zoology Building, Tillydrone Avenue, Aberdeen, AB24 2TZ, UK.

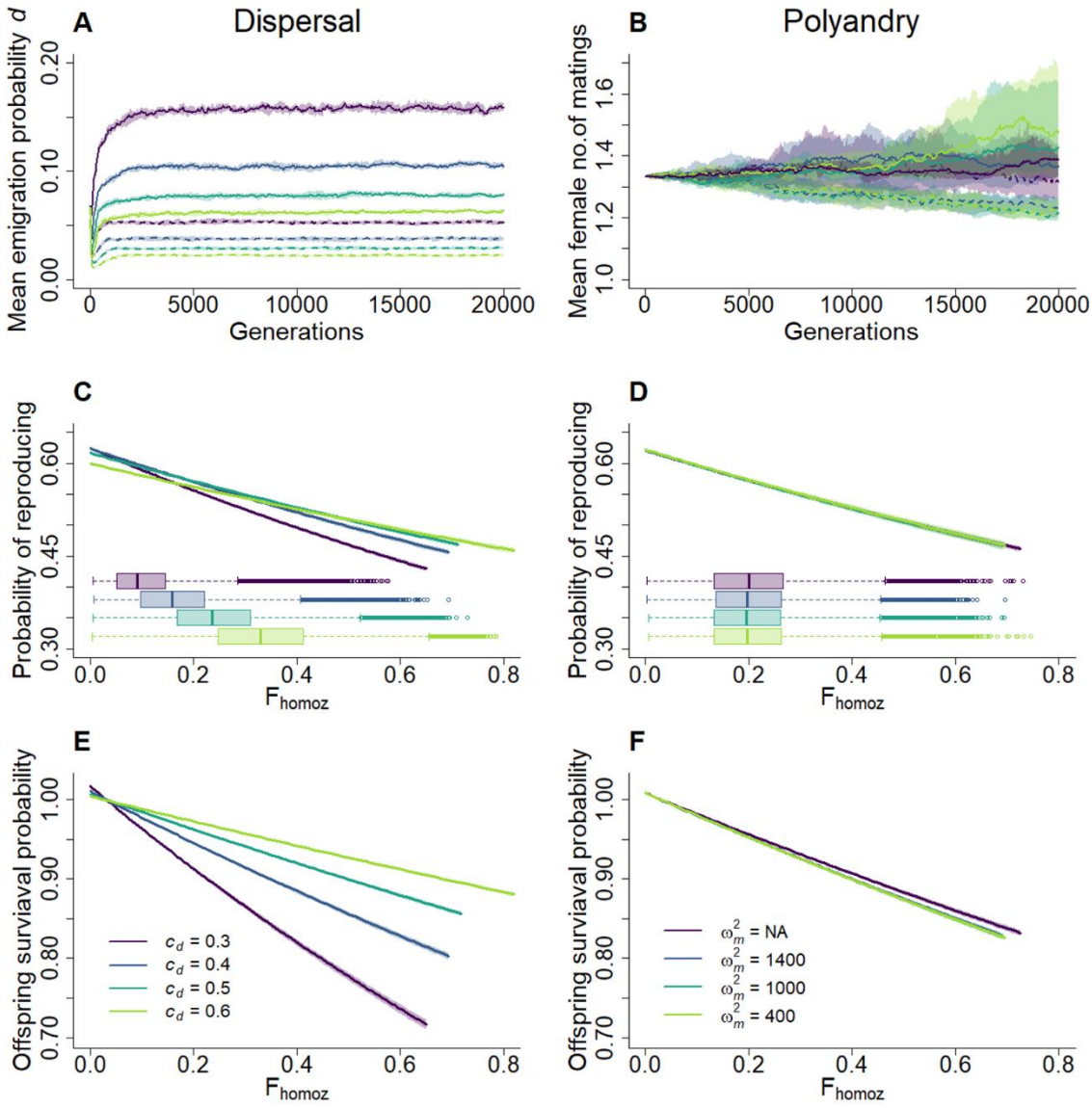

Figure S1. Effect of lower rate of deleterious mutations (U_d = 0.5; U_l = 0.1) on the evolution of dispersal and polyandry when either one or the other trait evolves. A) Evolution of mean dispersal probability phenotypes *d* in the absence of polyandry (*a* = 3.0), under different costs of dispersal (c_d = 0.3, 0.4, 0.5, 0.6), in the absence (dashed lines) or presence (solid lines) of deleterious mutations. **B)** Evolution of mean polyandry phenotypes (expected female number of matings, *P* = 1 + 1/*a*) evolved under fix dispersal probability (*d* = 0.05), as a function of different strengths of direct selection against female remating (no cost; $\boldsymbol{\omega_m^2}$ = 1400, 1000, 400) in the absence (dashed lines) or presence (solid lines) of deleterious mutations. In A-B, lines represent the median of mean phenotypes across 20 replicate simulations; colored shades depict the first and third quartile. The color legend for panels A,C,E is presented in E; the legend for panels B,D,F

802 is presented in F. **C-D)** Relationship between individual probability of reproducing and inbreeding
803 coefficient F_{homoz} (i.e., ID in reproduction probability) when **C)** dispersal evolves under different
804 costs in the absence of polyandry and, **D)** polyandry evolves under different strengths of direct
805 selection with fix dispersal probability. Lines show the fitted models and colored shades the 95%
806 CI. Models are fitted at generation 20,000 to a subsample of 140 populations, across 10
807 replicates. Boxplots represents the distribution of the individual F_{homoz}. **E-F)** Relationship between
808 offspring survival probability and F_{homoz} (i.e., ID in offspring survival probability). In E simulation
809 scenarios and parameters as in C; in F as in D.
810

811

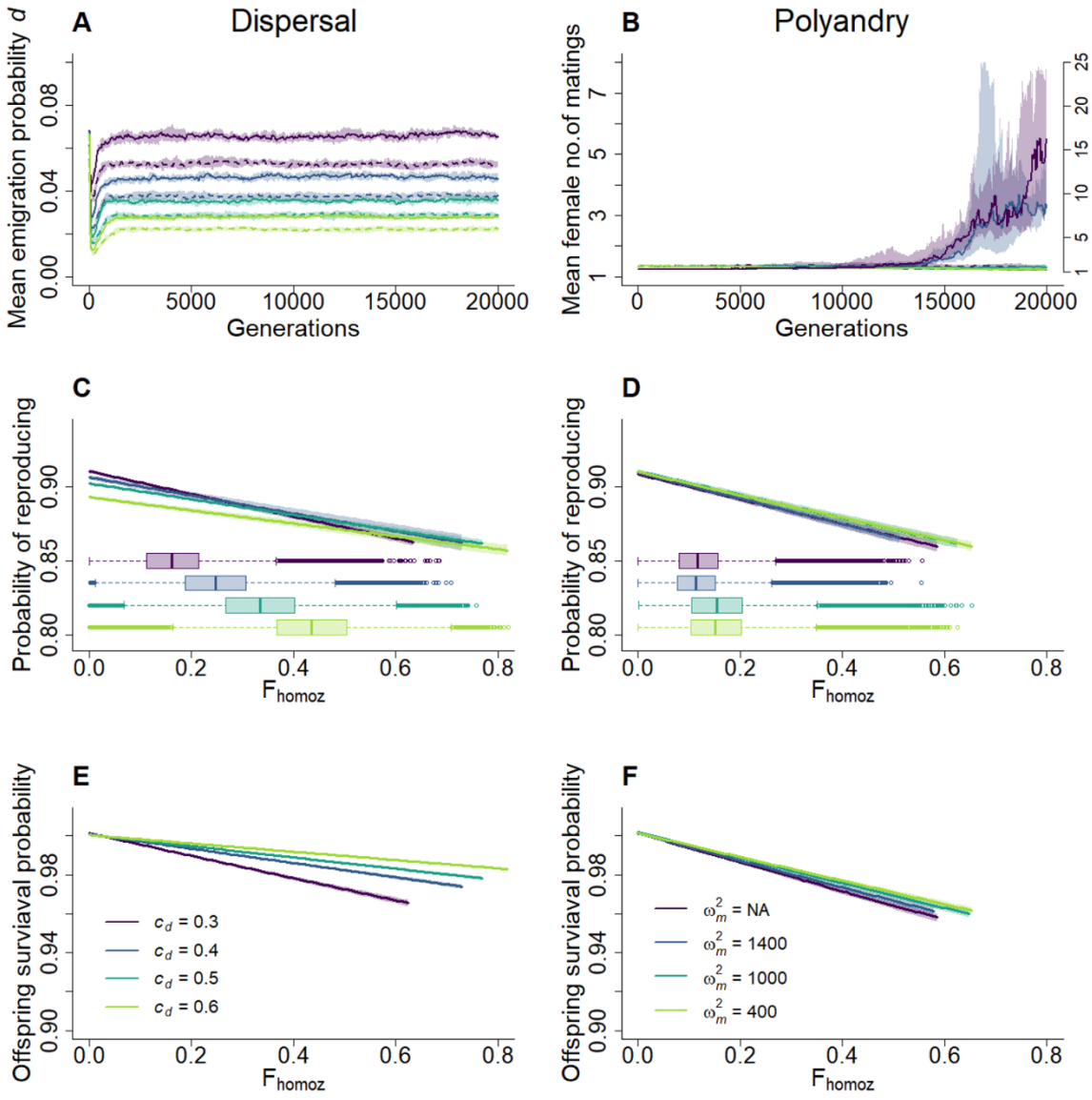

Figure S2. Effect of very low rate of deleterious mutations (U_d = 0.1; U_l = 0.02) on the evolution of dispersal and polyandry when either one or the other trait evolves. A) Evolution of mean dispersal probability phenotypes *d* in the absence of polyandry (*a* = 3.0), under different costs of dispersal (c_d = 0.3, 0.4, 0.5, 0.6), in the absence (dashed lines) or presence (solid lines) of deleterious mutations. B) Evolution of mean polyandry phenotypes (expected female number of matings, *P* = 1 + 1/*a*) evolved under fix dispersal probability (*d* = 0.05), as a function of different strengths of direct selection against female remating (no cost; $\boldsymbol{\omega_m^2}$ = 1400, 1000, 400) in the absence (dashed lines) or presence (solid lines) of deleterious mutations. In A-B, lines represent the median of mean phenotypes across 20 replicated simulations; colored shades depict the first and third quartile. The color legend for panels A,C,E is presented in E; the legend for panels B,D,F is presented in F. C-D) Relationship between individual probability of reproducing and inbreeding

coefficient F_{homoz} (i.e., ID in reproduction probability) when C) dispersal evolves under different costs in the absence of polyandry and, D) polyandry evolves under different strengths of direct selection with fix dispersal probability. Lines show the fitted models and colored shades the 95% CI. Models are fitted at generation 20,000 to a subsample of 140 populations, across 10 replicates. Boxplots represents the distribution of the individual F_{homoz}. E-F) Relationship between offspring survival probability and F_{homoz} (i.e., ID in offspring survival probability). In E simulation scenarios and parameters as in C; in F as in D.

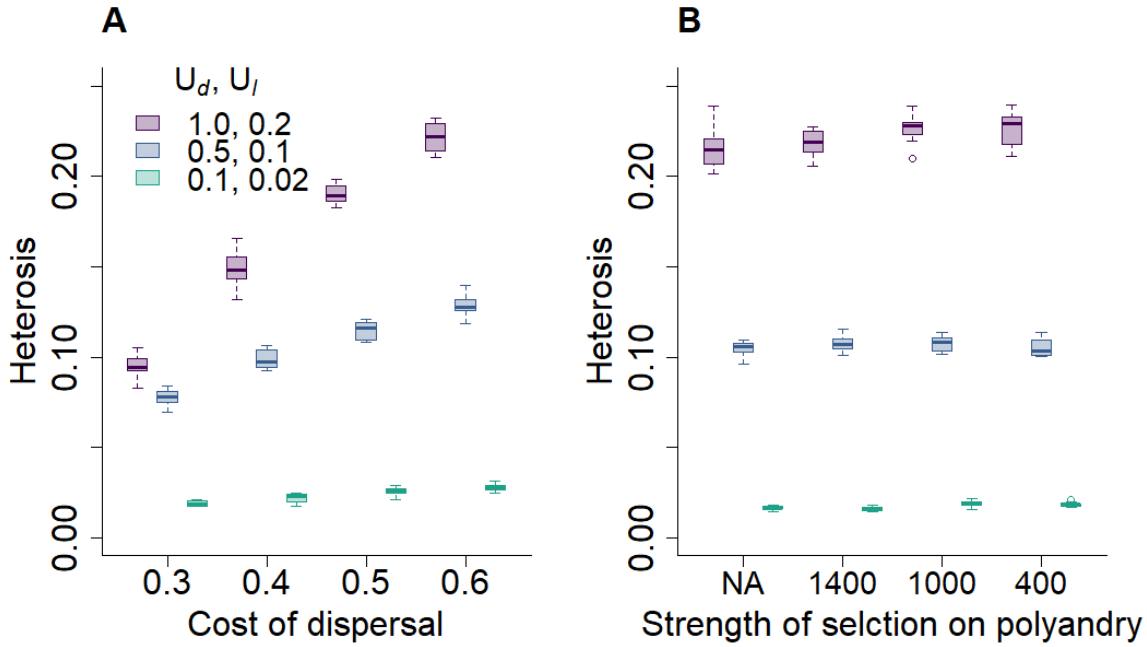

Figure S3. Heterosis emerging when either dispersal or polyandry evolve under different rates of deleterious mutations. A) Heterosis as a function of cost of dispersal c_d and different rates of mildly deleterious (U_d) and lethal (U_l) mutations (colors), when only dispersal is evolving in the absence of polyandry. B) Heterosis as a function of the strength of direct selection against polyandry $\boldsymbol{\omega_m^2}$ and different rates deleterious mutations, when only polyandry is evolving under fix dispersal probability (d = 0.05). Heterosis is shown as median (solid bands), first and third quartiles (box limits), and approximately twice the standard deviation (whiskers) over 20 replicate simulations at generation 20,000.

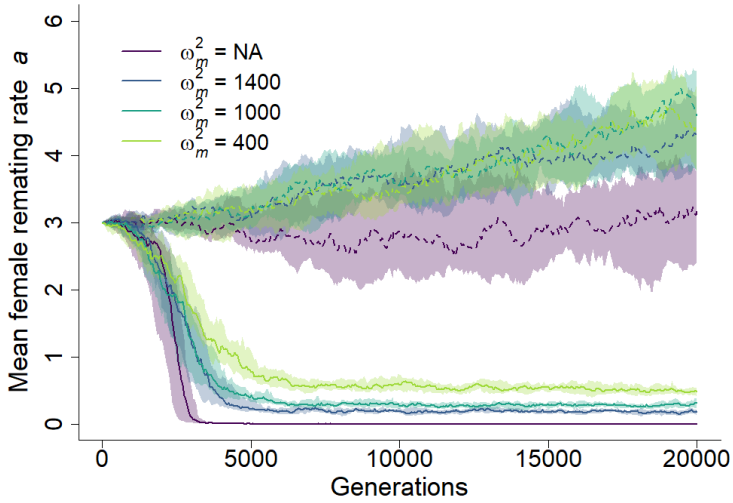

Figure S4. Evolution of female re-mating rate *a* under fix dispersal. Evolution of mean female remating rate phenotypes (*a*) under fix dispersal probability (*d* = 0.05), as a function of different strengths of direct selection against female remating (no cost; $\boldsymbol{\omega_m^2}$= 1400, 1000, 400) in the absence (dashed lines) or presence (solid lines) of deleterious mutations. Lines represent the median of mean phenotypes across 20 replicated simulations; colored shades depict the first and third quartile. Other parameters: U_d = 1.0; U_l = 0.2.

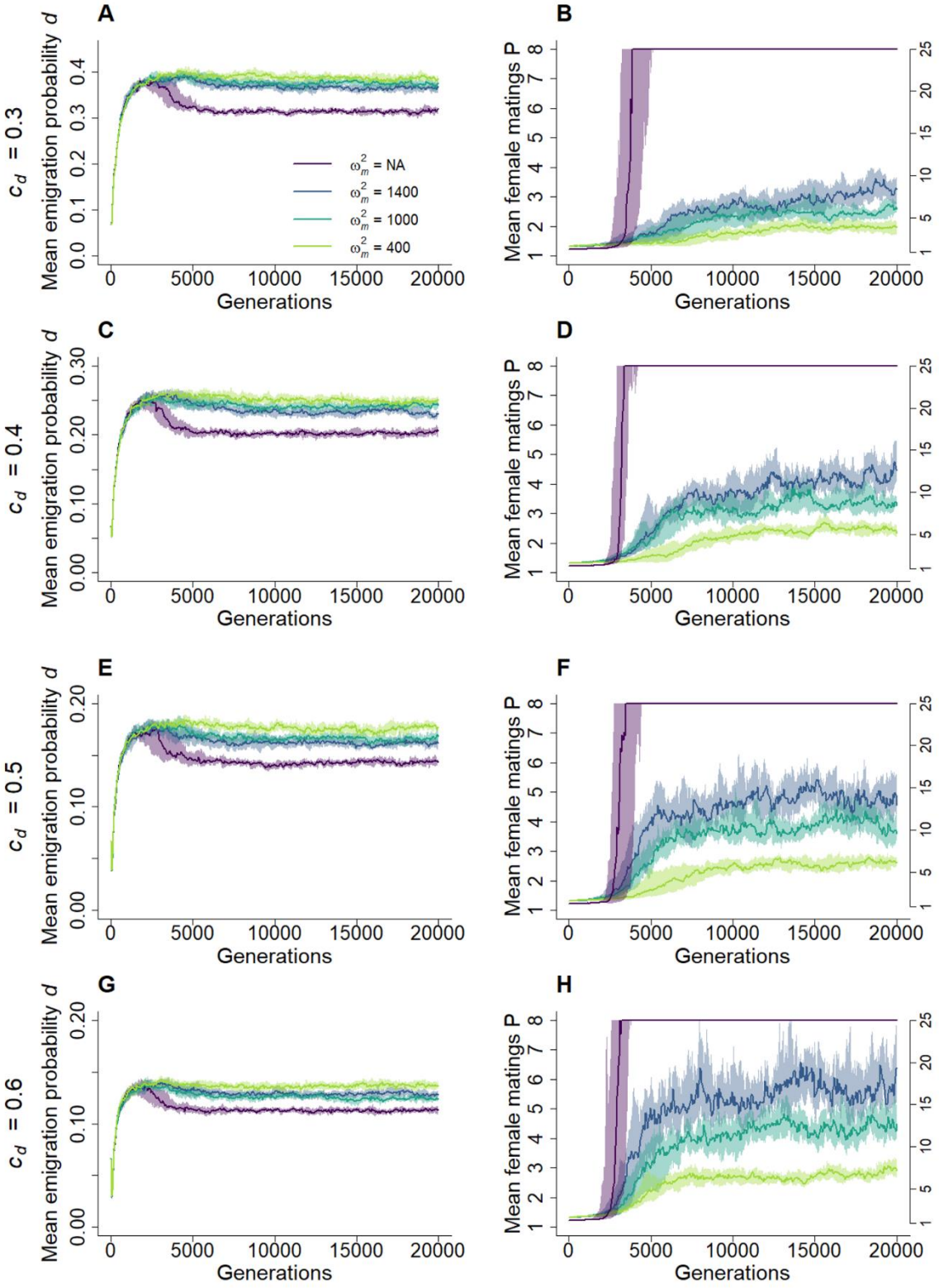

851

852 **Figure S5 (previous page). Evolutionary dynamics of dispersal and polyandry.** Joint
853 evolution of mean dispersal probability phenotypes (*d*) and mean polyandry phenotypes (expect
854 female number of matings: $P = 1 + 1/a$) in the presence of deleterious mutation, given different
855 costs of dispersal c_d (**A-B:** 0.3; **C-D:** 0.4; **E-F:** 0.5; **G-H:** 0.6) and different strengths of direct
856 selection against female re-mating (no cost; $\boldsymbol{\omega_m^2}$= 1400, 1000, 400, depicted by different colors).
857 In the absence of direct selection against polyandry ($\boldsymbol{\omega_m^2}$= NA), females evolved to mate with all
858 the males in the population; the y-axis on the right hand-side refers to this single line (purple).
859 Lines represent the median of mean phenotypes across 20 replicated simulations; colored shades
860 depict the first and third quartile.
861

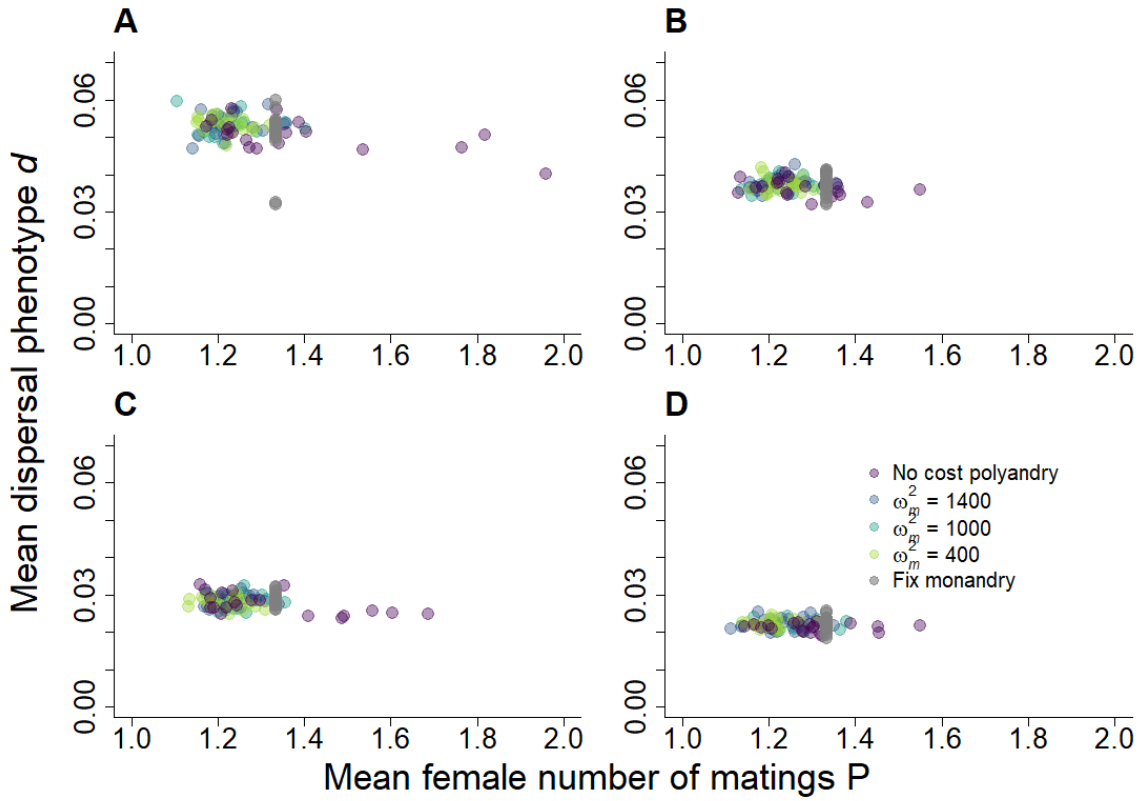

Figure S6. Joint evolution of dispersal and polyandry in the absence of inbreeding depression. Mean dispersal probability phenotypes (*d*) and mean polyandry phenotypes (expected female number of matings: $P = 1 + 1/a$) in the absence of deleterious mutations, given different costs of dispersal c_d (**A:** 0.3; **B:** 0.4; **C:** 0.5; **D:** 0.6) and different strengths of direct selection against female re-mating (no cost; $\boldsymbol{\omega_m^2}$ = 1400, 1000, 400). Each data point represents the mean phenotypic values for one out of 20 replicate simulations at generation 20,000. Colored dots indicate simulations where dispersal and polyandry jointly evolved; grey dots, simulations where dispersal evolved given fix monandry ($a = 3.0$).

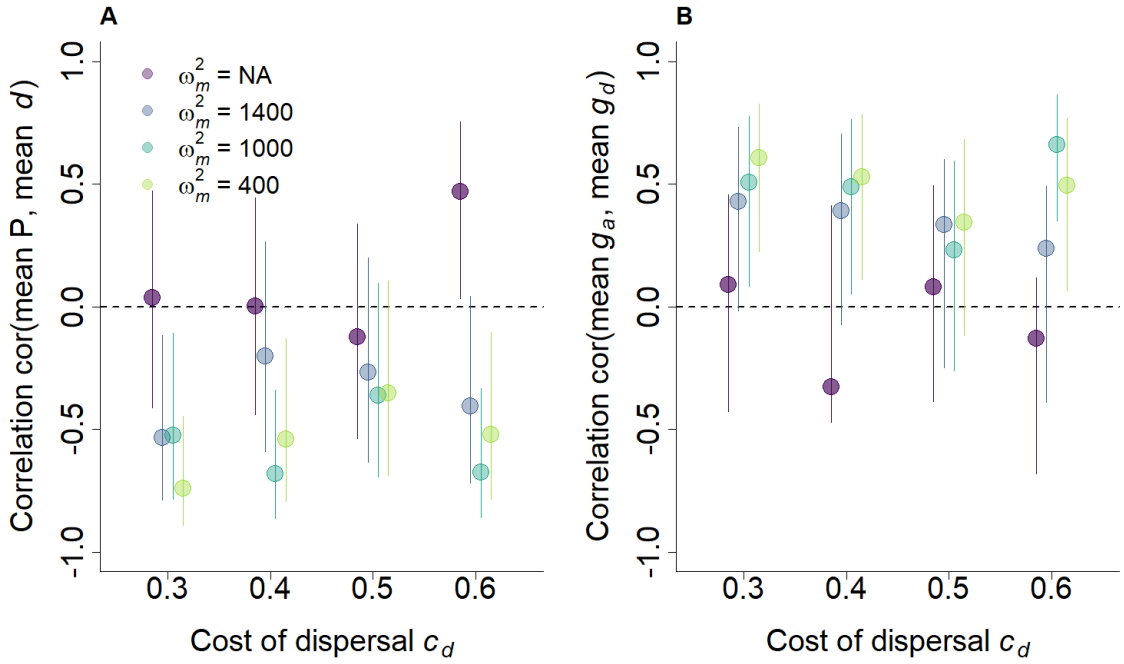

871

872 **Figure S7. Correlation between polyandry and dispersal at the metapopulation level. A)**
873 Correlation between mean polyandry phenotype ($P = 1 + 1/a$) and mean dispersal phenotype (d),
874 and **B)** correlation between mean genotypic female re-mating rate (g_a) and mean genotypic
875 dispersal (g_d), given different costs of dispersal c_d and different strengths of direct selection
876 against female re-mating (no cost; $\boldsymbol{\omega_m^2}$ = 1400, 1000, 400). Correlations are calculated across 20
877 replicate simulations between each replicate mean phenotypic and genotypic values. Means are
878 calculated across all individuals in the metapopulation and over the last 500 generations. Bars
879 represents the 95% confidence intervals.

880

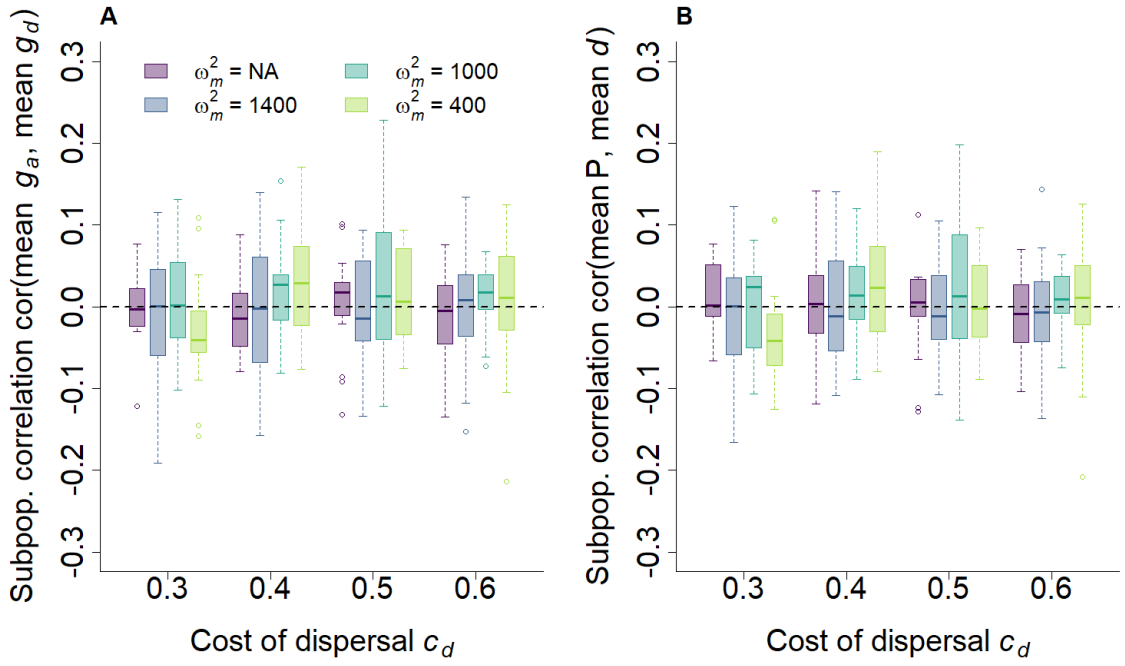

881

882 **Figure S8. Absence of between subpopulation correlation between polyandry and**
883 **dispersal. A)** Correlation between mean genotypic female re-mating rate (g_a) and mean
884 genotypic dispersal (g_d), and **B)** between mean polyandry phenotype (P = 1 + 1/a) and mean
885 dispersal phenotype (d), given different costs of dispersal c_d and different strengths of direct
886 selection against female re-mating (no cost; $\boldsymbol{\omega_m^2}$ = 1400, 1000, 400). Correlations are calculated
887 for each replicate across subpopulations mean phenotypic and genotypic values at generation
888 20,000. Means are calculated across all individuals in each subpopulation. Correlations are
889 shown as median (solid bands), first and third quartiles (box limits), and approximately twice the
890 standard deviation (whiskers) over 20 replicate simulations.

891

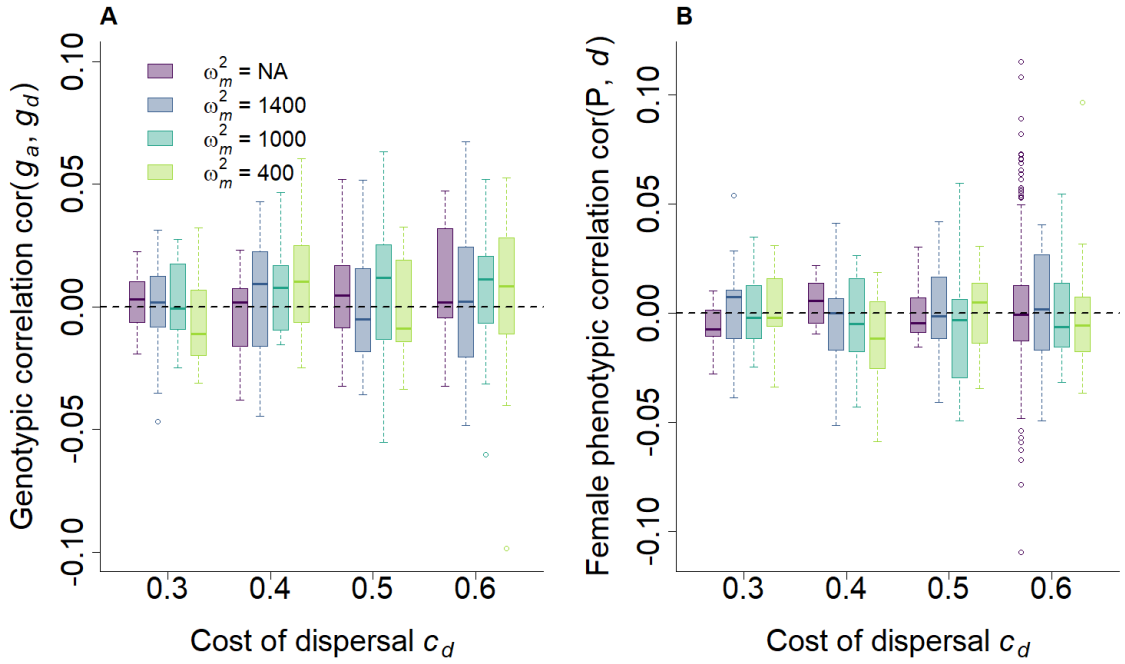

892

893 **Figure S9. Absence of genetic correlation between polyandry and dispersal. A)** Genetic
894 correlation between female re-mating rate genotypic value (g_a) and dispersal genotypic value (g_d),
895 and **B)** genetic correlation between female polyandry phenotype (P = 1 + 1/a) and female
896 dispersal phenotype (d), given different costs of dispersal c_d and different strengths of direct
897 selection against female re-mating (no cost; $\boldsymbol{\omega_m^2}$ = 1400, 1000, 400). Correlations are calculated
898 for each replicate across individuals phenotypic and genotypic values at generation 20,000, and
899 are shown as median (solid bands), first and third quartiles (box limits), and approximately twice
900 the standard deviation (whiskers) over 20 replicate simulations.

901

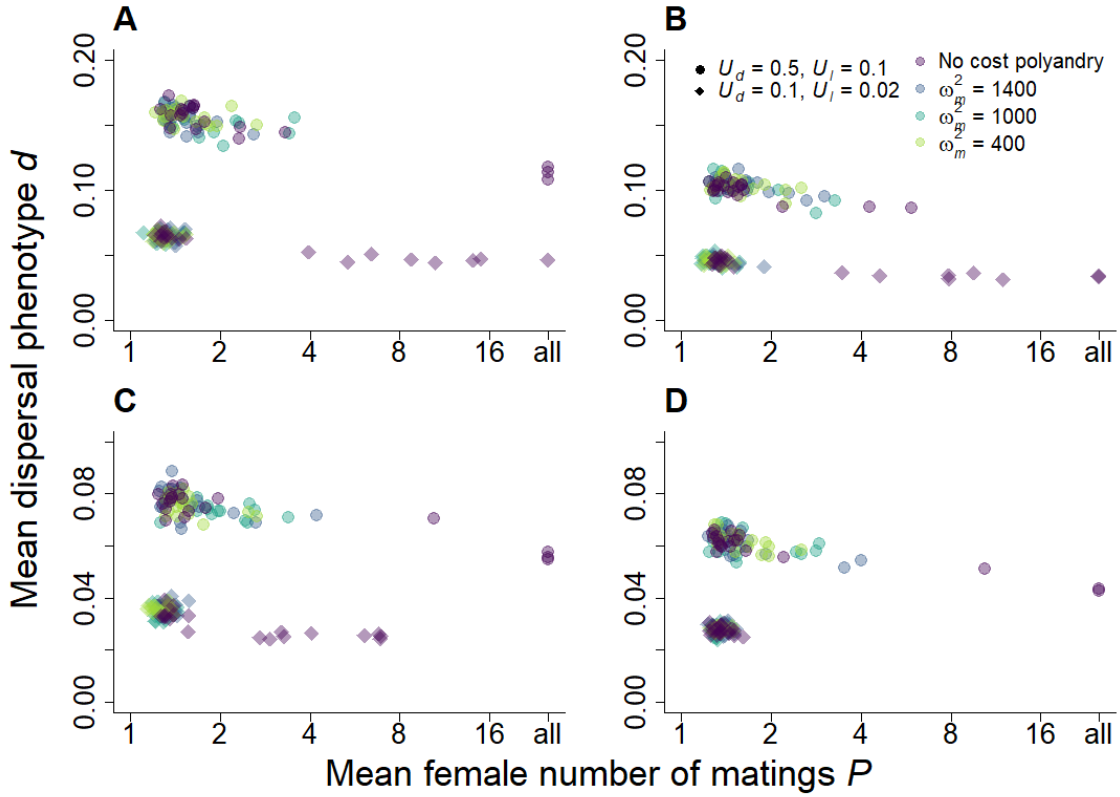

902

903 **Figure S10. Effect of lower deleterious mutation rate on the joint evolution of dispersal and**
904 **polyandry.** Joint evolution of mean dispersal probability phenotypes (*d*) and mean polyandry
905 phenotypes (expect female number of matings: $P = 1 + 1/a$) at two different levels of deleterious
906 mutation rates, given different costs of dispersal c_d (**A:** 0.3; **B:** 0.4; **C:** 0.5; **D:** 0.6) and different
907 strengths of direct selection against female re-mating (no cost; ω_m^2= 1400, 1000, 400). Dots
908 represent simulations where U_d = 0.5 and U_l = 0.1, while diamonds represent simulations where
909 U_d = 0.1 and U_l = 0.02, thus corresponding to mutation rates that are half and a tenth, respectively,
910 of the mutation rates presented in the main results (Fig. 2). Each data point represents the mean
911 phenotypic value for one out of 20 replicate simulations at generation 20,000. The x-axis is on the
912 logarithmic scale to aid visualization.

913

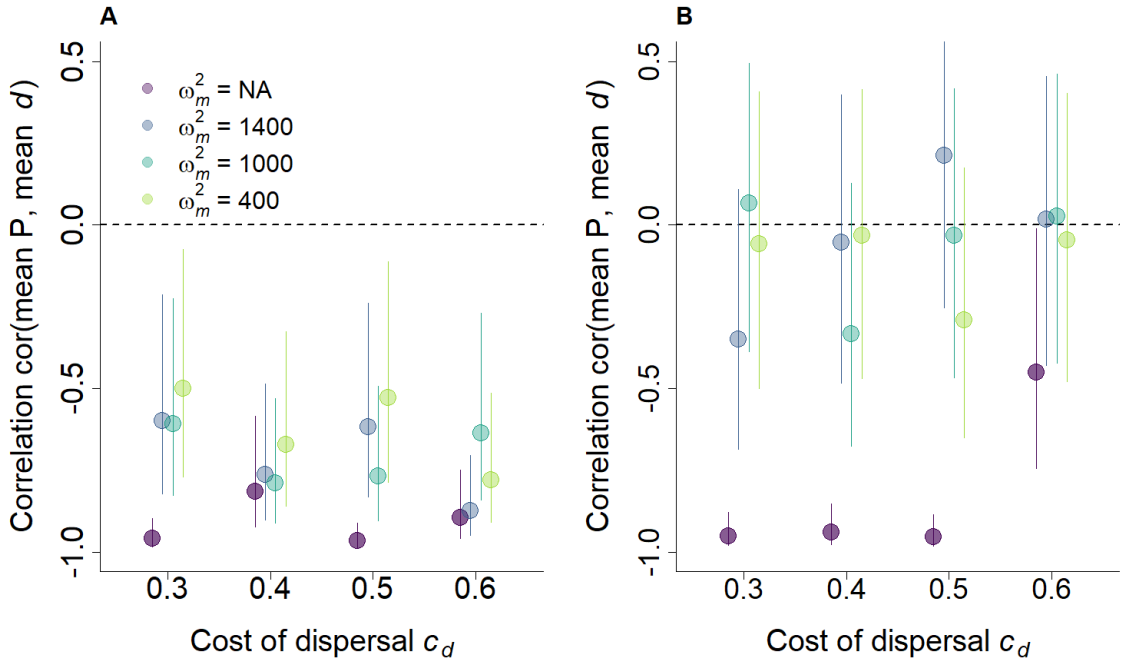

914

915 **Figure S11. Correlation between polyandry and dispersal at the metapopulation level for**
916 **lower rates of deleterious mutations**. Correlation between mean polyandry phenotype (*P* = 1
917 + 1/*a*) and mean dispersal phenotype (*d*) given **A)** U_d = 0.5 and U_l = 0.1, and **B)** U_d = 0.1 and U_l
918 = 0.02. Results are presented for different costs of dispersal c_d and different strengths of direct
919 selection against female re-mating (no cost; ω_m^2 = 1400, 1000, 400). Correlations are calculated
920 across 20 replicate simulations between each replicate mean phenotypic and genotypic values.
921 Means are calculated across all individuals in the metapopulation and over the last 500
922 generations. Bars represents the 95% confidence intervals.

923

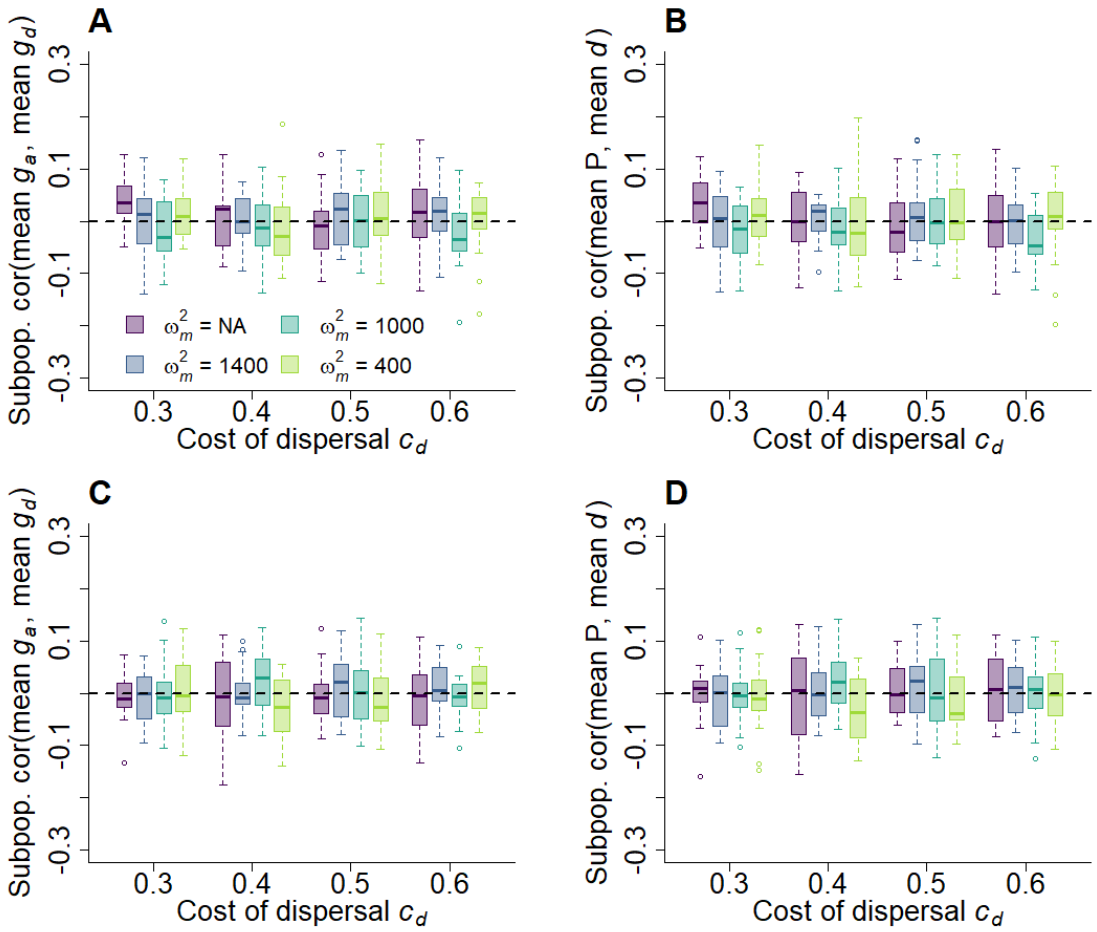

Figure S12. Correlation between polyandry and dispersal at the subpopulation level for lower rates of deleterious mutations. **A)** Correlation between mean genotypic female re-mating rate (g_a) and mean genotypic dispersal (g_d), and **B)** between mean polyandry phenotype (P = 1 + 1/a) and mean dispersal phenotype (d), given different costs of dispersal c_d and different strengths of direct selection against female re-mating (no cost; ω_m^2 = 1400, 1000, 400), when mutation rates U_d = 0.5 and U_l = 0.1. **C-D)** same as A-B, but when U_d = 0.1 and U_l = 0.02. Correlations are calculated for each replicate across subpopulations mean phenotypic and genotypic values at generation 20,000. Means are calculated across all individuals in each subpopulation. Correlations are shown as median (solid bands), first and third quartiles (box limits), and approximately twice the standard deviation (whiskers) over 20 replicate simulations.

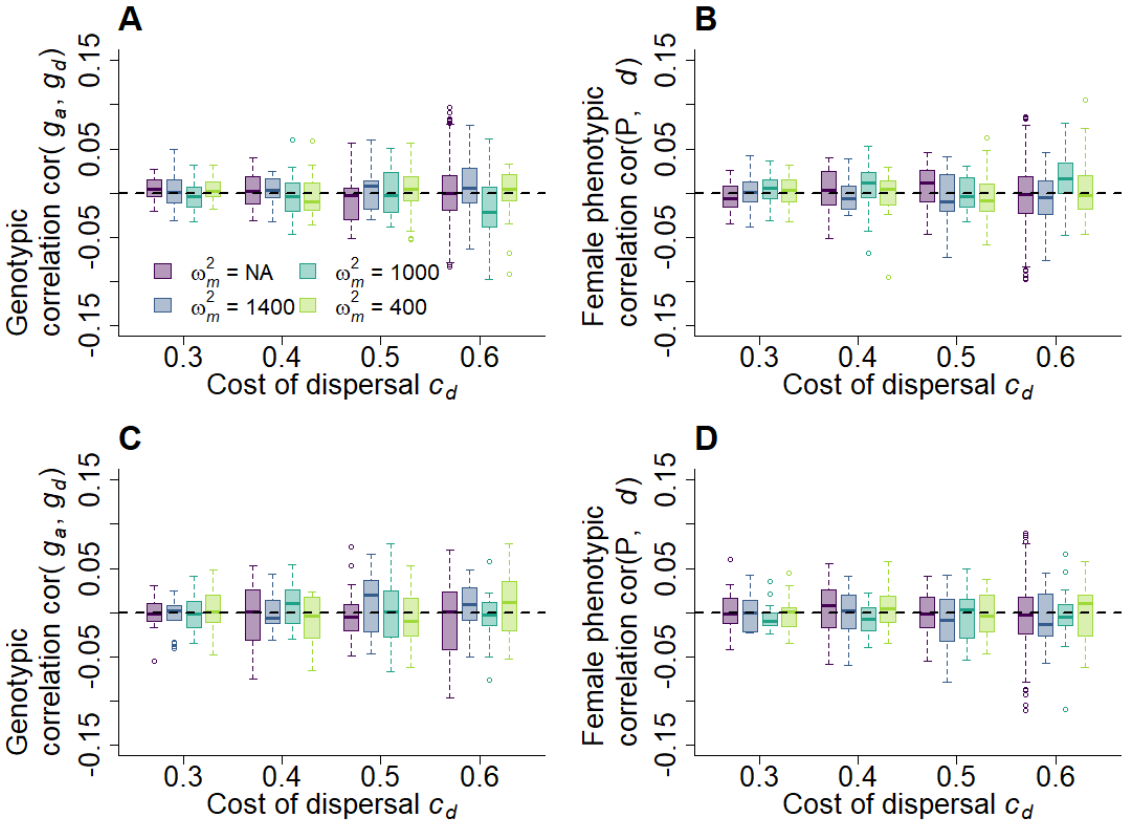

Figure S13. Genetic correlation between polyandry and dispersal for lower rates of deleterious mutations. **A)** Genetic correlation between female re-mating rate genotypic value (g_a) and dispersal genotypic value (g_d), and **B)** genetic correlation between female polyandry phenotype ($P = 1 + 1/a$) and female dispersal phenotype (d), given different costs of dispersal c_d and different strengths of direct selection against female re-mating (no cost; ω_m^2 = 1400, 1000, 400), when mutation rates $U_d = 0.5$ and $U_l = 0.1$. **C-D)** same as A-B, but when $U_d = 0.1$ and $U_l = 0.02$. Correlations are calculated for each replicate across individuals phenotypic and genotypic values at generation 20,000, and are shown as median (solid bands), first and third quartiles (box limits), and approximately twice the standard deviation (whiskers) over 20 replicate simulations.

946 **Table S1.** Model variables and parameters.

Variables	Description	Parameter values
K	Carrying capacity per cell (sub-population)	50 individuals
f	Female fecundity	12
Inbreeding and inbreeding depression		
R	Genome map length (for the continuous chromosome carrying deleterious mutations)	10
s	Selection coefficient of mildly deleterious mutations	$\Gamma(\alpha, {}^{s_d}/_{\alpha})$
h	Dominance coefficient of mildly deleterious mutations	$\mathrm{U}[0.0, e^{-ks}]$
s_d	Mean selection coefficient of mildly deleterious mutations	0.05
h_d	Mean dominance coefficient of mildly deleterious mutations	0.3
α	Shape parameter of gamma distribution of s	1.0
k	Constant	$-\log(2h_d)/s_d$
s_l	Selection coefficient of lethal mutations	1.0
h_l	Dominance coefficient of lethal mutations	0.02
U_d	Mutation rate for mildly deleterious mutations	1[1], 0.5, 0.1 / diploid genome / generation
U_l	Mutation rate for lethal mutations	0.2*, 0.1, 0.02 / diploid genome / generation
L_n	Number of neutral diploid loci	500
	Neutral allelic values	$\mathrm{U}[-1000.0,1000.0]$
F_{homoz}	Individual neutral homozygosity (proxy for inbreeding coefficient)	
r	Recombination rate for neutral loci	0.1
μ_n	Mutation probability for neutral alleles	0.001 / haploid locus / generation
Traits		
L	Number of diploid loci for each trait	1
a	Female re-mating interval (phenotypic value)	$a \geq 0.0$
d	Emigration probability (phenotypic value)	$0.0 \leq d \leq 1.0$
	Initial genotypic mean for female re-mating rate	3.0

[1] Values used in the simulations presented in the main text.

	Initial genotypic mean for emigration probability	0.05
$\sigma^2_{a,0}$	Initial genotypic variance for female re-mating rate	0.25
$\sigma^2_{d,0}$	Initial genotypic variance for emigration probability	0.1
μ	Mutation probability	0.001 / haploid locus / generation
	Mutational effects	$N(0.0, 0.07)$
Costs		
ω^2_m	Strength of direct selection against female multiple mating	no cost, 1400, 1000, 400
c_d	Cost of dispersal	0.3, 0.4, 0.5, 0.6

947

Table S2. Coefficients (i.e., mutation load β_0, and inbreeding load β_1) and relative standard errors of the relationship between individual probability of reproducing and inbreeding coefficient F_{homoz}, and between offspring survival probability and F_{homoz}. Results are presented for simulations where dispersal evolves under different costs (c_d), in the absence of polyandry, and where polyandry evolves under different strengths of direct selection (ω_m^2), with fix dispersal probability. Models are fitted at generation 20,000 to a subsample of 140 populations, across 10 replicates.

	Probability of reproducing				***Offspring survival***			
Only dispersal evolving								
C_d	β_0	**SE**	β_1	**SE**	β_0	**SE**	β_1	**SE**
0.3	-0.99	0.005	-1.34	0.016	0.11	0.001	-1.97	0.025
0.4	-0.94	0.003	-1.16	0.018	0.07	0.001	-1.29	0.014
0.5	-0.92	0.005	-0.98	0.016	0.04	0.001	-0.78	0.008
0.6	-0.92	0.002	-0.79	0.014	0.02	0.0004	-0.52	0.005
Only polyandry evolving								
ω_m^2	β_0	**SE**	β_1	**SE**	β_0	**SE**	β_1	**SE**
none	-0.94	0.004	-0.81	0.007	0.02	0.0003	-0.49	0.005
1400	-0.94	0.003	-0.79	0.014	0.02	0.0003	-0.46	0.005
1000	-0.94	0.003	-0.78	0.009	0.02	0.0003	-0.46	0.005
400	-0.94	0.003	-0.77	0.009	0.02	0.0003	-0.46	0.005

Table S3. Jointly evolving dispersal and polyandry affect evolution of inbreeding depression in reproduction and survival. Coefficients (i.e., mutation load β_0, and inbreeding load β_1) and relative standard errors of the relationship between individual probability of reproducing and inbreeding coefficient F_{homoz}, and between offspring survival probability and F_{homoz}, when dispersal and polyandry are jointly evolving. Results are presented for varying costs of dispersal (c_d) and strengths of direct selection against female multiple mating (ω_m^2). Models are fitted at generation 20,000 to a subsample of 140 populations, across 10 replicates.

		Probability of reproduction				***Survival probability***			
C_d	ω_m^2	β_0	**SE**	β_1	**SE**	β_0	**SE**	β_1	**SE**
0.3	**none**	-0.99	0.003	-1.29	0.024	0.07	0.001	-1.74	0.023
	1400	-0.99	0.002	-1.35	0.022	0.09	0.001	-1.90	0.024
	1000	-0.99	0.003	-1.34	0.020	0.09	0.001	-1.86	0.024
	400	-0.99	0.004	-1.35	0.017	0.09	0.001	-1.87	0.024
0.4	**none**	-0.95	0.003	-1.09	0.035	0.04	0.001	-1.10	0.013
	1400	-0.95	0.001	-1.14	0.016	0.05	0.001	-1.20	0.014
	1000	-0.95	0.004	-1.17	0.014	0.05	0.001	-1.22	0.014
	400	-0.95	0.002	-1.17	0.019	0.06	0.001	-1.20	0.014
0.5	**none**	-0.94	0.003	-0.93	0.014	0.03	0.0004	-0.72	0.008
	1400	-0.93	0.002	-0.96	0.018	0.03	0.0004	-0.76	0.008
	1000	-0.93	0.003	-0.91	0.013	0.03	0.0004	-0.74	0.008
	400	-0.93	0.003	-0.99	0.011	0.04	0.0005	-0.78	0.008
0.6	**none**	-0.94	0.002	-0.77	0.012	0.02	0.0003	-0.46	0.005
	1400	-0.93	0.001	-0.80	0.012	0.02	0.0003	-0.50	0.005
	1000	-0.94	0.003	-0.80	0.012	0.02	0.0003	-0.49	0.005
	400	-0.93	0.004	-0.80	0.011	0.03	0.0003	-0.52	0.006